

# Probing Enzyme Phosphoester Interactions by Combining Mutagenesis and Chemical Modification of Phosphate Ester Oxygens

James T. Stivers\* and Rajesh Nagarajan

Department of Pharmacology and Molecular Sciences, Johns Hopkins University School of Medicine, 725 North Wolfe Street, Baltimore, Maryland 21205

Received January 12, 2006

## Contents

1. Introduction	3443	7.4.2. Combining Bridging and Nonbridging Phosphorothioate Substitution with Mutagenesis	3464
1.1. Importance of the Phosphoester Handle in Biological Systems	3443	7.5. Protein Tyrosine Phosphatase	3464
1.2. Chemical Substitutions at Phosphate Ester Oxygens	3444	7.5.1. Nonbridging Phosphorothioate Substitution and Mutagenesis	3464
1.3. Scope	3444	8. Concluding Remarks	3465
2. Noncovalent Interactions with Phosphate Esters	3446	9. Abbreviations	3465
2.1. Hydrogen Bonding	3446	10. Acknowledgments	3465
2.2. Electrostatic Effects	3447	11. References	3465
2.3. Sterics and Flexibility	3447		
3. Chemical Reactivity of Phosphoester, Phosphothioester, and Phosphonoester Linkages	3447		
4. Free Energy Analysis: Combining Mutagenesis and Chemical Modification	3449		
5. Experimental Techniques	3450		
5.1. Modified Substrates and Ligands	3450		
5.2. Key Considerations in Binding and Kinetic Measurements	3451		
6. Examples Using Chemical Modification of Phosphate Esters Alone	3451		
6.1. Protein–RNA Binding Reactions	3451		
6.2. Reactions with DNA: <i>EcoRI</i> and <i>EcoRV</i> Restriction Enzymes	3453		
7. Examples Combining Chemical Modification and Mutagenesis	3455		
7.1. RNase T <sub>1</sub>	3455		
7.1.1. Nonbridging Phosphorothioate Substitution and RNase T <sub>1</sub> Mutagenesis	3455		
7.2. Vaccinia DNA Topoisomerase I (VTopo)	3456		
7.2.1. Bridging Phosphorothioate Substitution and VTopo Mutagenesis	3457		
7.2.2. Dissecting the Energetics of Nonbridging Phosphorothioate Substitution with VTopo Mutants	3458		
7.2.3. Structural Interpretations	3458		
7.2.4. Methylphosphonate Substitution and VTopo Mutagenesis	3459		
7.3. Uracil DNA Glycosylase	3460		
7.3.1. Nonbridging Phosphorothioate Substitution near the Deglycosylation Site	3461		
7.3.2. Nonbridging Methylphosphonate Substitution near the Deglycosylation Site	3462		
7.4. Phosphoinositol-Specific Phospholipase C	3463		
7.4.1. Nonbridging Phosphorothioate Substitution and Mutagenesis	3464		

## 1. Introduction

### 1.1. Importance of the Phosphoester Handle in Biological Systems

Proteins, nucleic acids, lipids, and various other smaller biomolecules are united by the presence of a common chemical entity of paramount and unique importance—the phosphate ester. In proteins, phosphomonoester groups are added as reversible post-translational modifications to serine, threonine, or tyrosine amino acid side chains, and they serve as a switch for intracellular signaling cascades (phosphoserine, phosphothreonine, or phosphotyrosine).<sup>1</sup> Alternatively, phosphoamide linkages involving the nitrogens of histidine or lysine side chains serve as high energy phosphoryl donors in multistep phosphoryl transfer reactions (Figure 1A).<sup>2</sup> In nucleic acids, the phosphodiester linkage provides the exceptionally stable polymeric backbone upon which the coding information of the nucleic acid bases is carried (Figure 1B). In this regard, the biological selection of phosphate ester linkages for long-term information storage in DNA may in part reside in their resistance to hydrolysis ( $t_{1/2} = 30$  million years)<sup>3</sup> and in the requirement for a charged linkage that promotes aqueous solubility and deters aggregation. In phospholipids, the negatively charged phosphate monoester head group imbues phospholipid bilayers with their aqueous affinity that is crucial for forming functional cell membranes (Figure 1C). Finally, phosphorylated polyalcohols such as inositol play a key role in intracellular signaling cascades that allow regulation of a diverse array of cellular processes (Figure 1D).<sup>4</sup> Because the phosphate ester group is used in numerous ways in biology, a detailed molecular understanding of the interactions of proteins, enzymes, and small molecules with these ubiquitous functional groups is of great interest.

The primary focus of this review is enzymes that interact with phosphate esters to promote catalysis. These interactions may be divided into two general classes: indirect and direct.

\* Phone: 410-502-2758. Fax: 410-955-3023. E-mail: jstivers@jhmi.edu.



James T. Stivers was born in Philadelphia, PA, and raised in Anchorage, Alaska. After pursuing a music degree from Berklee College of Music in Boston and serving as a staff composer/arranger for the Air Force Band for several years, he received a B.S. in Microbiology and Immunology from the University of Washington in 1987. He obtained his Ph.D. in Biochemistry in 1992 from Johns Hopkins University, where he became interested in enzyme catalysis. He received postdoctoral training in heteronuclear NMR and enzymology in the laboratory of Professor Albert Mildvan at Johns Hopkins Medical School, where he was an American Cancer Society postdoctoral fellow from 1993 to 1996. He then joined the faculty of the Center for Advanced Research in Biotechnology in Rockville, MD, as an Assistant Professor in 1996. During the year 2001, he moved his laboratory to the Department of Pharmacology and Molecular Sciences at Johns Hopkins Medical School, where he is now an Associate Professor. Presently, his research focuses on understanding the nature of enzyme catalysis and inhibition for a number of enzymes involved in DNA repair and recombination. When time allows, he still enjoys playing both the classical and electric guitars.



Rajesh Nagarajan was born in Madras, India. He earned a B.Sc. degree in Chemistry from Madras Christian College, India, and subsequently received a master's degree in 1998 from the Indian Institute of Technology, Madras. He did his graduate research on bacterial resistance enzymes in the laboratory of Dr. Rex F. Pratt at Wesleyan University. After receiving his Ph.D. in 2004, he moved to The Johns Hopkins University School of Medicine to do postdoctoral research in topoisomerase enzymology under the supervision of Dr. James T. Stivers. He has recently accepted a tenure track position at Skidmore College, beginning this fall.

The indirect interaction involves noncovalent bonding of the enzyme to an oxygen atom of a phosphate ester group that does not undergo a change in covalent bonding during the enzymatic reaction (Figure 2). By definition, indirect interactions must involve substrates (such as DNA and RNA) that contain more than one phosphate ester group, and the specific binding energy of the enzyme with such groups can be used to drive catalysis in a variety of ways, as discussed in detail below. In contrast, the direct interaction (at least within the scope of this review) involves noncovalent bonding to a

phosphate ester center that is the direct target of a nucleophilic substitution reaction (Figure 2). In terms of catalysis, both indirect and direct interactions can have comparable, large effects in lowering the activation barrier for a given reaction. As will be illuminated throughout this review, the dense display of lone pair electrons on the phosphate ester oxygens, and the overall negative charge of the phosphate ester group provide unique opportunities for powerful hydrogen bonding and electrostatic interactions that may be used to either destabilize ground states or stabilize transition states, as required for enzymatic catalysis (Figure 2).<sup>5</sup>

## 1.2. Chemical Substitutions at Phosphate Ester Oxygens

One general goal in the field of chemical biology and enzymology is to develop chemical tools that can provide unique insights into the nature of protein–ligand interactions that go beyond those provided by structural methods such as X-ray crystallography or NMR spectroscopy. The idealized objective is to construct chemical congeners of naturally occurring biological functional groups that discretely probe one energetic aspect of an interaction. Thus, the change in a binding interaction of the congener in the ground state and transition state relative to the actual functional group provides a measure of the energetic importance and the nature of the native interaction. Of course, truly selective perturbations of a single interaction are seldom if ever realized, and one is always faced with the harsh reality that observed energetic perturbations to such complex systems as enzyme–substrate complexes will always be a mixture of short-range and long-range effects brought about by the cooperative nature of the binding interactions. Nevertheless, chemical perturbation approaches can be qualitatively and quantitatively useful if binding measurements are made for each stable complex along a reaction coordinate and the structures of the complexes are also available. Moreover, as is the major focal point of this review, combining chemical perturbation approaches with protein mutagenesis can provide more compelling insights than either approach alone.

Frequently used congeners for phosphate diesters are shown in Figure 3 (analogous congeners can be made for monoesters and triesters of phosphate). The depicted chemical substitutions may be divided into two classes depending on whether a nonbridging or bridging oxygen is replaced. Stereospecific substitution of a nonbridging oxygen with sulfur or a methyl group is often performed to explore the importance of hydrogen bonding, steric fit, or electrostatic interactions with a specific oxygen. Contrastingly, substitution of a low  $pK_a$  sulfur for a bridging oxygen is assumed to destabilize the ester linkage to nucleophilic attack by relinquishing the requirement for acid catalysis of expulsion of the high  $pK_a$  oxygen leaving group. The chemical rationale for these effects of nonbridging and bridging substitutions is discussed in detail in section 2. We also note here that substitution of a single nonbridging oxygen of a prochiral phosphate diester with another atom or functional group generates a stereocenter as depicted in Figure 3.

## 1.3. Scope

The literature where oxygen atoms of phosphate esters have been substituted to investigate properties of various biological systems is extensive and dates back at least 45 years.<sup>6</sup> This review focuses on studies that have used sulfur

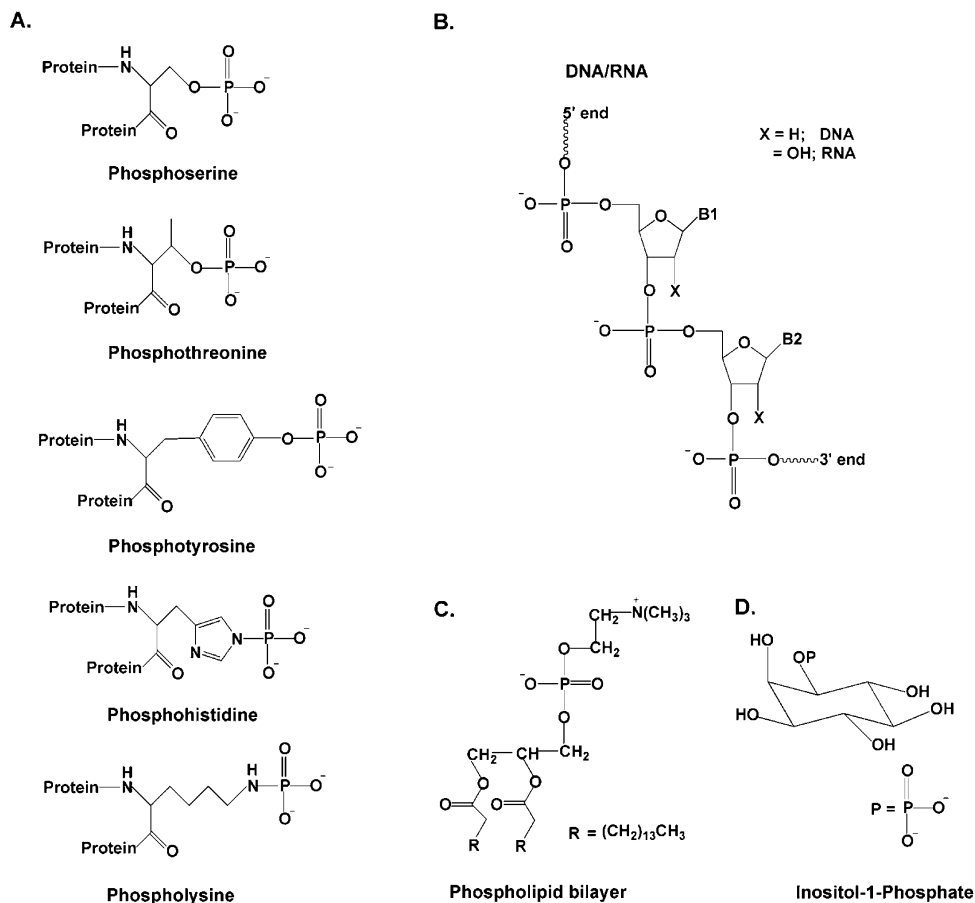


**Figure 1.** Various biological forms of phosphate esters: (A) phosphorylated amino acids; (B) nucleic acids; (C) phospholipids; (D) inositol-1-phosphate.

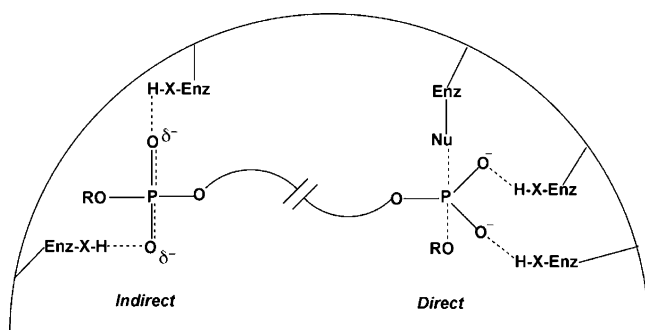


**Figure 2.** Examples of indirect and direct catalytic interactions of an enzyme with phosphate ester groups. The direct interaction (right) involves a phosphate group that undergoes nucleophilic substitution during the course of the enzymatic reaction. Hydrogen bonding groups (H–X) are used to stabilize the charge development in a pentacoordinate transition state. Indirect noncovalent interactions with a phosphate ester (left) can be used to position a substrate, to electrostatically destabilize a ground state, or to stabilize a transition state. Many examples of catalytically important indirect interactions are found in sections 6 and 7.

and carbon substitution of phosphate ester oxygens to probe the energetics of protein–ligand interactions, with a deliberate emphasis on enzymatic reactions. Notably, we specifically exclude studies in which the phosphate ester oxygen is coordinated to a metal ion in favor of systems where the enzyme itself makes direct contact with the phosphate ester. In this regard, studies using nucleotides fall outside this scope,<sup>7–9</sup> and we refer the reader to elegant studies that cover the powerful approach of “metal rescue” in which the

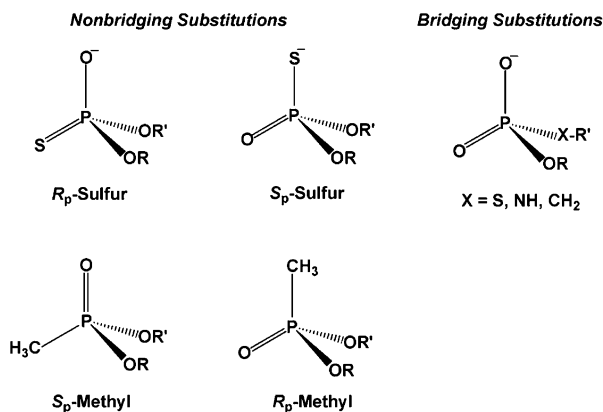


**Figure 3.** Common nonbridging and bridging chemical substitutions of oxygen atoms of phosphate esters. In this figure, the stereochemical priority is  $R > R'$ .

damaging effect of sulfur substitution for oxygen is ameliorated by switching to a soft metal that prefers bonding to sulfur.<sup>10–12</sup> In addition, the general approach of using stereospecific sulfur substitution to determine the stereochemical course of enzymatic nucleophilic substitution reactions is not covered to any significant extent and we refer the reader elsewhere for this methodology.<sup>8,6,13</sup> Our approach is to first provide an overview of the chemical basis for the energetic effects of sulfur and methyl substitution for oxygen, then present the free energy analysis that describes the combined energetic effects of phosphate ester substitution and mutagenesis, and finally, provide representative examples that exemplify the utility of the approach.

## 2. Noncovalent Interactions with Phosphate Esters

A compelling interpretation of an observed energetic effect arising from substitution of an oxygen atom of a phosphate ester with sulfur or a methyl group requires careful consideration of the nature of the chemical perturbation and, if possible, the structure of the protein-bound ligand. Although the following section critically presents the possible outcomes of such substitutions, in practice, the observed energetic effects often are quite unambiguous with respect to identifying important enzyme–oxygen contacts. Very often, careful studies that combine both chemical substitution and protein mutagenesis can provide interaction maps at various steps along a reaction coordinate that can be as detailed as structural studies. Most importantly, direct experimental evidence for transition-state interactions can be revealed, whereas these contacts can only be indirectly inferred from structural studies.

### 2.1. Hydrogen Bonding

Substitution of sulfur or a methyl group for a nonbridging oxygen of a phosphate ester is expected to have a significant effect on hydrogen bond enthalpy, but the net free energy effect of the substitution is difficult to predict because even these fairly conservative replacements result in complex changes to the system. For instance, sulfur substitution preserves the overall charge of the group, but sulfur has lower electronegativity than oxygen, which would be expected to lead to weaker hydrogen bonding because the strength of hydrogen bonds is largely dependent on the magnitudes of the charges on the donor and acceptor groups.<sup>5,14</sup> These differences between phosphate esters and phosphothioesters may be easily visualized as electrostatic potentials plotted on the van der Waals surfaces of these groups (Figure 4). However, this simple expectation based on electronegativity differences is complicated by the fact that the negative charge of a phosphomonoester and diester linkage is evenly delocalized between all nonbridging oxygen atoms, whereas P–S bonds have less double bond character in aqueous solution as judged by NMR chemical shift and  $pK_a$  data<sup>15</sup> and, therefore, possess a greater net negative charge than a given nonbridging phosphate ester oxygen.<sup>15</sup> However, it should be pointed out that crystallographic data<sup>16</sup> and quantum mechanical calculations<sup>17</sup> have indicated that the P–O and P–S bond orders are both close to 1.5, with somewhat greater negative charge on oxygen than sulfur. The previous computational result is recapitulated in the DFT/B3LYP/6-31G\* electrostatic potentials for the phosphorothioate dimethyl ester shown in Figure 4B. The reasons for these discrepancies between solution, crystallographic, and computational methods remain unclear. Further compounding quantitative predictions of the energetic outcome of sulfur substitution is the fact that hydrogen bonds are strongest when the  $pK_a$  values of the donor and acceptor are matched.<sup>5,18,19</sup> Thus, without detailed knowledge of the proton affinities of the donor and acceptor groups in the protein microenvironment, it is exceedingly difficult to predict net energetic effects of sulfur substitution. Despite potential complications in the meaningful interpretation of sulfur substitution effects, we will see from numerous real examples that very useful insights into hydrogen bonding interactions can typically be gleaned from such studies. When unexpected energetic outcomes arise from sulfur substitution, these too

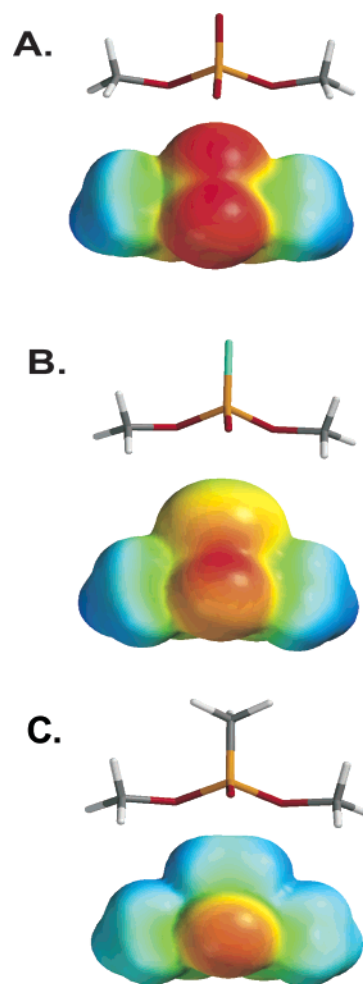


**Figure 4.** Lowest energy structures and electrostatic potential energy surfaces for esters of dimethyl phosphate substituted with sulfur or  $\text{CH}_3$  at a nonbridging oxygen: (A) dimethyl ester of phosphate; (B) dimethyl ester of thiophosphate; (C) dimethyl ester of methylphosphonate. Geometries and electrostatic potentials were calculated using Spartan04 using DFT/B3LYP/6-31G\*.

can elucidate subtle properties of the system, especially if structural information is also available.

Substitution of a methyl group for a nonbridging oxygen of a phosphate diester presents a somewhat simpler situation in terms of possible energetic outcomes with respect to hydrogen bond donors. The most obvious effects arising from this substitution are the complete ablation of negative charge and the substitution of a functional group ( $\text{CH}_3$ ) that has no lone pair electrons for accepting hydrogen bonds (Figure 4C).<sup>17</sup> Accordingly, stereospecific substitution of a methyl group for oxygen would be expected to give rise to a larger damaging effect than the analogous sulfur substitution. Despite the apparent straightforward nature of stereospecific methyl substitution, it must be realized that oxygen replacement removes the negative charge that is delocalized over both nonbridging oxygens, and therefore, the effect is not strictly stereospecific. In addition, methyl substitution on a nonbridging atom also makes the charge on the bridging oxygen atom more electropositive than that in a phosphate ester. This effect arises because of the increased electrophilicity of the phosphorus atom that in turn increases the bond order to the bridging oxygen atoms. These outcomes have ramifications for interpretation as presented in the discussion below pertaining to electrostatics.



The final and most mechanistically informative phosphate diester substitution is the replacement of a bridging oxygen leaving group with sulfur. The power of this chemical perturbation resides in the dramatically lower  $pK_a$  value of a thiolate leaving group ( $pK_a \sim 8$ ) as compared to oxygen ( $pK_a \sim 15$ )<sup>20</sup> and in the smaller bond dissociation energy of the P–S bond relative to the P–O bond ( $\sim 50$  and  $100$  kcal/mol, respectively),<sup>21</sup> both of which increase the leaving group potential of bridging thiophosphate esters. For nucleophilic substitution reactions that have largely dissociative character, lowering the  $pK_a$  of the leaving group can have a profound effect on the reaction rate.<sup>22</sup> As described below, the excellent leaving group ability of sulfur provides the basis for the powerful “sulfur rescue” methodology, one of the most unambiguous approaches for identifying an enzyme amino acid side chain that serves as a proton donor (general acid) to the poorer oxygen leaving group (see section 7.2.2).

## 2.2. Electrostatic Effects

One of the most important aspects of phosphate monoester and diester linkages is their negative charge, which can be a powerful recognition feature especially in a low dielectric environment such as that often found in enzyme active sites. Thus, it is useful to consider the possible electrostatic consequences of sulfur or methyl substitution for a nonbridging oxygen. For simplicity, we consider a phosphate diester linkage with a formal charge of  $-1$ , but similar considerations would hold for a monoester with a charge of  $-2$  at neutral pH. Since hydrogen bonds can involve charged groups and are themselves electrostatic in nature,<sup>18</sup> we explicitly define an electrostatic interaction as involving a charged group greater than about  $3.5$  Å from the negatively charged oxygen. According to Coulomb’s law (eq 1), the

$$E = q_1 q_2 / \epsilon r \quad (1)$$

energy ( $E$ ) of such an interaction will show an inverse dependence on the effective dielectric constant ( $\epsilon$ ) and the distance ( $r$ ) between the two groups with effective charges  $q_1$  and  $q_2$ . This simple equation provides a useful basis for understanding electrostatic effects upon sulfur or methyl substitution, and it reveals some limitations for interpreting observed effects. Accordingly, we make the following general conclusions:

(i) *The magnitude of the electrostatic effect will depend on the change in effective charge on each nonbridging atom or group in the phosphate ester upon substitution with sulfur or a methyl group.* It may be reasonably assumed that in a solution the single negative charge on a phosphate diester is evenly delocalized over both nonbridging oxygens and (1) that this charge becomes more localized on sulfur upon substitution<sup>15</sup> and (2) that the charge is totally ablated upon methyl substitution. However, for protein environments, different scenarios can be envisioned. For instance, when one oxygen is interacting with a protein cationic group, the negative charge distribution will shift toward that oxygen. Thus, upon stereospecific substitution of sulfur for the interacting oxygen, there will be a smaller change in charge at that position than in aqueous solution, and in the absence of any other effects, the substitution may have little consequence on the binding interaction (Figure 5A). Similarly, substitution of the other noninteracting oxygen with sulfur may shift the charge density away from the oxygen that is involved in the electrostatic interaction and weaken

binding (Figure 5A). In the case of the methyl group, substitution of either nonbridging oxygen will ablate the charge, leading to the prediction that long-range electrostatic interactions may show no stereoselectivity, while direct hydrogen bonding interactions may show a strong stereoselective effect of methyl substitution (Figure 5B).

(ii) *The magnitude of the electrostatic effect upon substitution will depend on the change in distance between the effective charge on the nonbridging atom and a charged protein group.* The length of the P–O bond ( $1.51$  Å) is considerably shorter than the P–S bond ( $1.97$  Å), but it is nearly identical to the P–C bond ( $1.49$  Å) (see models in Figure 4).<sup>17</sup> Therefore, in terms of distance effects only and assuming that no steric conflicts are present, sulfur substitution may make a charged interaction stronger.

(iii) *The magnitude of the electrostatic effect will depend on whether the dielectric constant of the protein binding pocket remains unchanged upon substitution.* A common simplifying assumption in this methodology is that the dielectric environment of the protein does not change when the oxygen, sulfur, or methyl substituent is bound. Of course, this is not directly testable, and if waters of hydration are changed between the free and bound ligand or protein, or if structural rearrangements arise from substitution, then unexpected outcomes could result that complicate the interpretation.

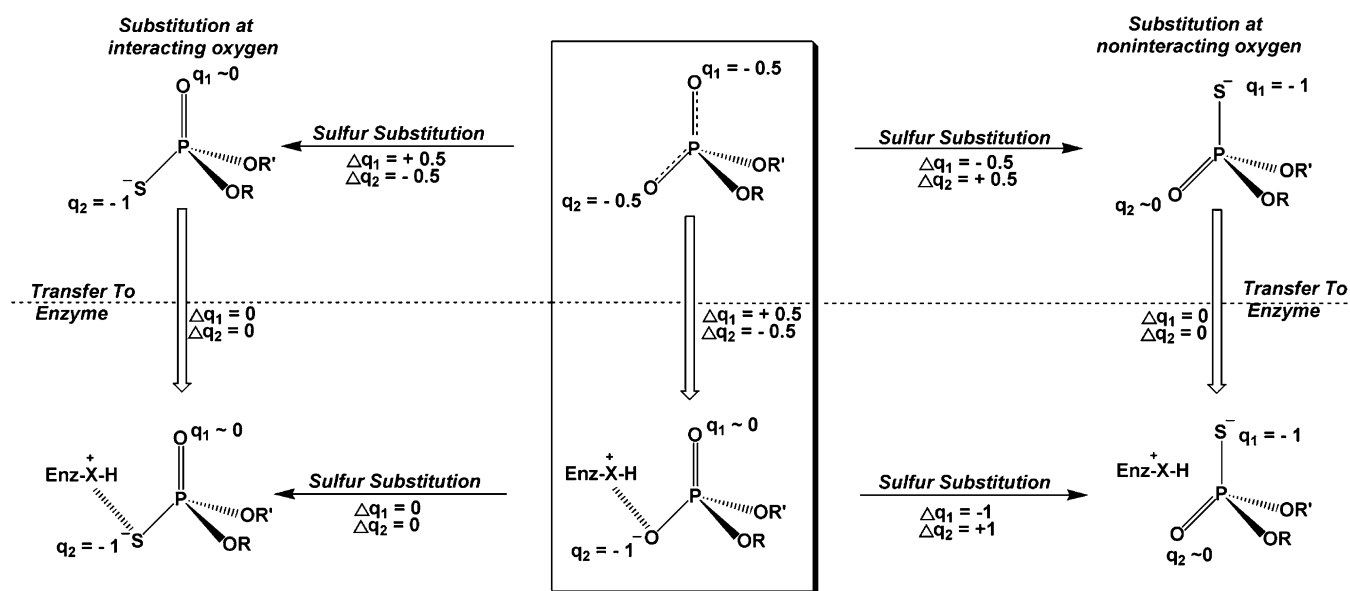
## 2.3. Sterics and Flexibility

The final aspects of methyl and sulfur substitution that should be considered are the differences in sterics and flexibility of the various esters. The van der Waals radius of a sulfur atom is considerably larger ( $1.85$  Å) than that of oxygen ( $1.44$  Å) whereas a methyl group is closer to isosteric ( $1.74$  Å).<sup>6,23</sup> Thus, sulfur substitution could give rise to stereospecific steric conflicts in an enzyme active site, whereas methyl substitution may not. In addition, increased double bond character would be expected for the other nonbridging oxygen upon sulfur and methyl substitution, leading to a shortening of this bond by about  $0.06$  Å.<sup>6,15</sup> Computational studies also indicate that there are differences in conformational flexibility of phosphate, phosphorothioate, and phosphonate esters that arise from aqueous solvation effects, hydrophobic interactions, and electrostatic and steric effects.<sup>17</sup> In particular, substitution of the 3’ or 5’ oxygen with sulfur in the phosphodiester linkage of DNA increases local flexibility as determined by computational approaches. In the context of duplex DNA, both methylphosphonate and phosphorothioate substitution can give rise to changes in the minor groove width (widening or narrowing),<sup>24</sup> hydration and cation localization in the minor groove,<sup>25,26</sup> and diastereomer specific changes in duplex stability.<sup>27,28</sup> Finally, it is well documented that methylphosphonate substitution in duplex DNA can result in dynamic bending of the duplex that presumably reflects the diminished charge repulsion of the backbone.<sup>24,29,30</sup>

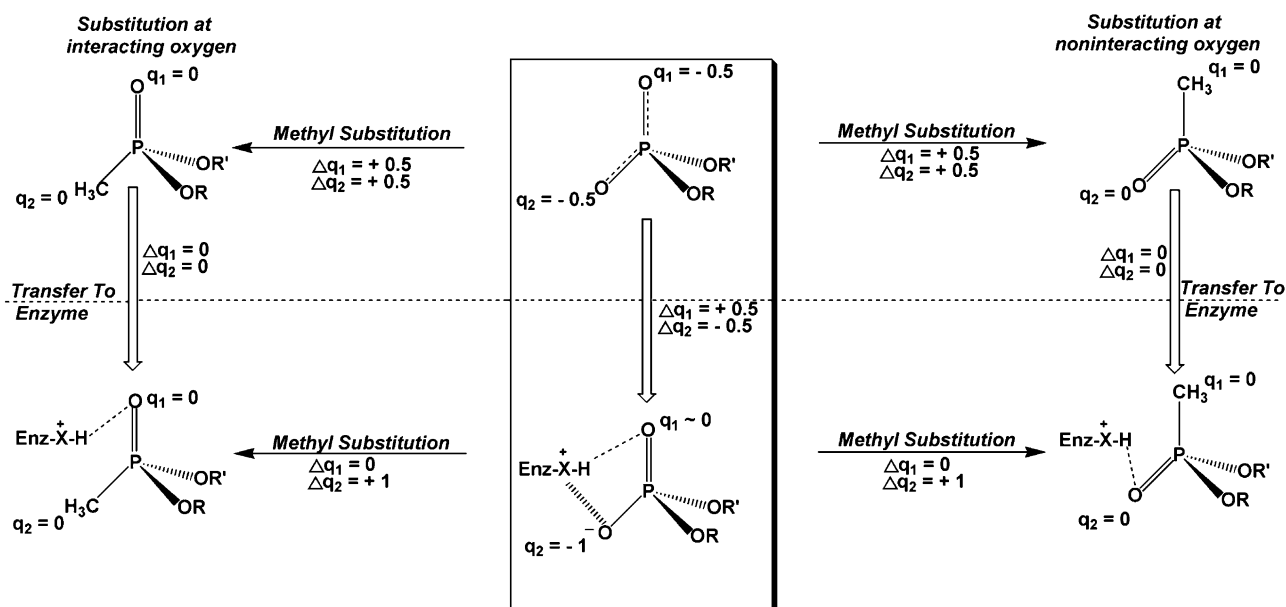
## 3. Chemical Reactivity of Phosphoester, Phosphothioester, and Phosphonoester Linkages

The transition-state structures for nucleophilic substitution at phosphorus centers of various phosphate esters have been extensively studied. We make no attempt to comprehensively review this important area, but instead, we refer the reader to other literature that covers this aspect of phosphate,<sup>31–38</sup>

## A. Sulfur Effects



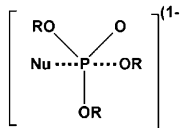
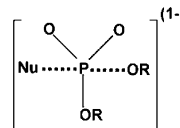
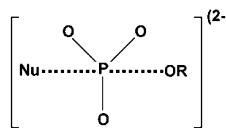
## B. Methyl Effects



**Figure 5.** Possible changes in charge of the nonbridging phosphate diester atoms upon substitution with sulfur or a methyl group in solution and in an enzyme active site. The charges shown on the atoms are approximate and are merely used for illustrating the possible effects. Two cases are depicted: one where the substituent interacts with an enzyme group (left) and one where the substituent does not interact (right). The effects on hydrogen bonding and electrostatics in an enzyme active site are depicted. (A) The center box shows the charge distribution of a phosphate diester in solution and upon transfer to an enzyme active site (vertical arrow). An enzyme cationic group ( $X-H^+$ ) is depicted that can serve as a charged hydrogen bond donor (hashed lines). Thus, the change in charge ( $\Delta q_2$ ) for the interacting oxygen upon transfer is  $-0.5$  whereas the other noninteracting oxygen shows a  $+0.5$  change ( $\Delta q_1$ ). Sulfur substitution for oxygen leads to accumulation of a full negative charge on S for both sulfur diastereomers (horizontal arrows, top). Unlike oxygen, a thio substituted position that interacts with a cationic enzyme group will feel little change in charge ( $\Delta q_2$  or  $\Delta q_1$ ), because sulfur is already carrying a full negative charge in solution (left vertical arrow). A similar analysis is shown for a noninteracting position (top, right vertical arrow). The net result is that nonbridging thio substitution in the context of the enzyme active site (horizontal arrows, bottom panel A) produces no changes in charge for the directly acting case (right) and large changes in charge for the noninteracting substitution. (B) An analogous scenario for methyl substitution.

phosphorothioate,<sup>39–42</sup> and phosphonate chemistry.<sup>43</sup> For our purposes, several general trends in the reactivity of these various esters are important to consider when making elemental substitution studies. First, reactions of phosphate esters show a systematic change in transition-state structure with monoesters being highly dissociative, triesters being

highly associative, and diesters having intermediate associative character (Figure 6),<sup>31–33,40</sup> Sulfur substitution for a nonbridging oxygen atom of these esters does not significantly change the transition-state structure for each of these reactions in solution,<sup>44</sup> but substantial changes in rate can occur. These “thio effects” on rate (defined as  $k^{ox}/k^s$ ) are

Phosphate Ester	$k^{\text{OX}}/k^{\text{S}}$	Transition State	$\beta_{\text{nu}}$	$\beta_{\text{lg}}$	Structure
Triester	10 - 160	Associative	0.3	-1.0	
Diester	4 - 11	Intermediate	0.3	-1.2	
Monoester	0.1 - 0.3	Dissociative	< 0.1	-1.2	

**Figure 6.** Nonbridging thio effects, transition-state structures, and nucleophile and leaving group dependencies for nucleophile substitution with various phosphate esters. See refs 31–42.

tabulated in Figure 6.<sup>40</sup> Notably, the nonbridging thio effect for a triester is about 25- and 1000-fold greater than those for a diester and monoester, respectively. These large differences have been reasonably attributed to the different transition-state structures for each ester and the electronegativity differences between oxygen and sulfur: the dissociative reaction of the monoester with an electron deficient phosphorus is accelerated by the greater electron donation from sulfur as compared to oxygen, whereas the associative reaction of the triester with an electron rich phosphorus is accelerated by the greater electron withdrawal by oxygen as compared to sulfur. Thus, enzymatic thio effects that differ significantly from these values suggest that other energetic contributions must be present (see above). Key issues with methylphosphonate diesters are that they are potentially more reactive than phosphate diesters and proceed by more associative triester-like mechanisms.<sup>43,45</sup> For instance, nucleophilic substitution by hydroxide ion is more than 10<sup>8</sup>-fold faster for a methylphosphonate diester than for the corresponding phosphate ester.<sup>43,46</sup>

#### 4. Free Energy Analysis: Combining Mutagenesis and Chemical Modification

The free energy changes in an enzyme–substrate binding interaction resulting from removal of an enzyme side chain, or upon substitution of a nonbridging oxygen atom with sulfur or a methyl group, may be analyzed using the same conceptual framework established for the effects of site-directed mutagenesis.<sup>47,48</sup> Since the binding interaction may be present in the ground-state Michaelis complex, the enzymatic transition state, or indeed any state of the enzyme bound substrate, it is possible to obtain interaction maps across an entire reaction pathway. With this formalism, the mutational difference free energies ( $\Delta\Delta G^{\text{mut}}$ ) are typically calculated from the ratio of a binding or kinetic parameter of the wild-type (wt) enzyme and the corresponding value for the mutated enzyme (mut). This is shown in eqs 2 and 3

$$\Delta\Delta G^{\text{mut}} = \Delta G^{\text{mut}} - \Delta G^{\text{wt}} = -RT \ln K_{\text{D}}^{\text{mut}}/K_{\text{D}}^{\text{wt}} \quad (2)$$

$$\Delta\Delta G^{\ddagger, \text{mut}} = \Delta G^{\ddagger, \text{mut}} - \Delta G^{\ddagger, \text{wt}} = -RT \ln k^{\text{mut}}/k^{\text{wt}} \quad (3)$$

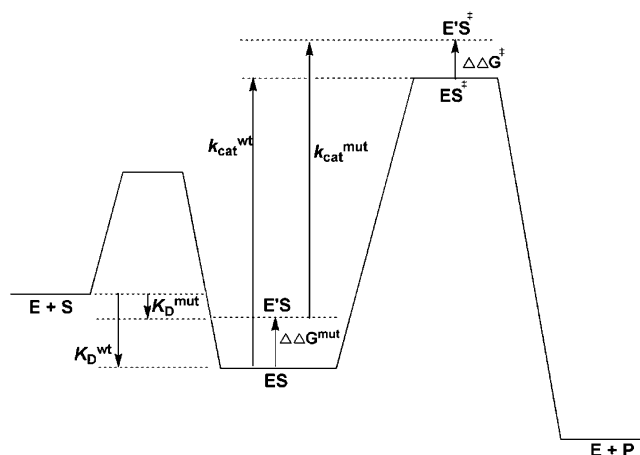


**Figure 7.** Free energy changes associated with binding ( $-RT \ln K_{\text{D}}$ ) and catalytic turnover ( $-RT \ln k_{\text{cat}}/\nu$ ) for a wild-type enzyme (wt) and a mutant form (mut). The difference free energies for binding of the mutant relative to the wild-type in the ground state ( $\Delta\Delta G^{\text{mut}}$ ) and the transition state are shown ( $\Delta\Delta G^{\ddagger}$ ). An identical diagram can be drawn for chemical substitution of an oxygen for sulfur or a methyl group. See text.

for an equilibrium binding measurement ( $K_{\text{D}}$ ), and a generic kinetic measurement ( $k$ ), where  $k$  could be  $k_{\text{cat}}$ ,  $k_{\text{cat}}/K_{\text{m}}$ , or even a single turnover kinetic constant for an enzyme. The difference free energies corresponding to a binding and  $k_{\text{cat}}$  measurement are depicted in the free energy reaction coordinate diagrams shown in Figure 7.

Similarly, in the case of chemical substitution, the difference free energies arising from the substitution ( $\Delta\Delta G^{\text{sub}}$ ) are calculated from the ratio of a binding or kinetic parameter for the oxygen containing substrate (ox) and the corresponding value for the substituted substrate (sub).

$$\Delta\Delta G^{\text{sub}} = \Delta G^{\text{ox}} - \Delta G^{\text{sub}} = -RT \ln K_{\text{D}}^{\text{ox}}/K_{\text{D}}^{\text{sub}} \quad (4)$$

$$\Delta\Delta G^{\ddagger, \text{sub}} = \Delta G^{\ddagger, \text{ox}} - \Delta G^{\ddagger, \text{sub}} = -RT \ln k^{\text{ox}}/k^{\text{sub}} \quad (5)$$

We next consider combining mutagenesis with chemical substitution, and the simplest possible expectations for how the substitution effect ( $\Delta\Delta G^{\text{sub}}$ ) changes upon removal of

an enzyme side chain that interacts with the substituted position. Substitution effects arise from a variety of factors that stem from the different size and electronic properties of the substituent as compared to oxygen. Typically, non-bridging substitution with sulfur or CH<sub>3</sub> gives rise to weaker binding interactions with an enzymatic group in the transition state (we will see numerous examples where this is not true in the ground state, however). In the simplest scenario, if an enzymatic group interacts directly with a nonbridging oxygen, then the substituent effect should be smaller for a mutant enzyme that lacks this group because the interaction was already lost by deletion of the side chain by mutagenesis (i.e.  $\Delta\Delta G^{\text{sub}} \rightarrow$  zero for the mutant). In contrast, if there is no change in the substitution effect for a mutant enzyme (i.e.  $\Delta\Delta G^{\text{sub}}$  is the same for the mutant and wild-type forms), then this provides evidence that the wild-type side chain does not interact with the given nonbridging oxygen (see below). Although mutation of a residue that interacts directly with the nonbridging atom would be expected to produce the largest change in the thio effect, significant changes may also occur if the mutated group alters the structure of the complex, thereby indirectly changing the interaction of the nonbridging oxygen with the enzyme. Thus, the interpretation of an altered thio effect upon mutagenesis is best done in conjunction with structural information.

In principle, the combined damaging effect of sulfur substitution and deleting an amino acid side chain ( $\Delta\Delta G^{\text{sub+mut}}$ ) can be the simple sum of the two individual effects ( $\Delta\Delta G^{\text{mut}} + \Delta\Delta G^{\text{sub}}$ ) or may differ from simple additivity by an amount termed the coupling energy ( $\Delta G_c$ , eq 6). In general,

$$\Delta\Delta G^{\text{sub+mut}} = \Delta\Delta G^{\text{mut}} + \Delta\Delta G^{\text{sub}} + \Delta G_c \quad (6)$$

a coupling energy will be observed when either of the single alterations changes the interaction energy between the mutated residue and the substitution site. We note, but do not derive, that the coupling energy may be calculated in a straightforward way from the ratio of the substitution effect ( $k^{\text{ox}}/k^{\text{sub}}$ ) for the wild type and mutated enzyme forms (eq 7). Obviously, a direct interaction between an enzyme group

$$\Delta G_c = -RT \ln (k^{\text{ox}}/k^{\text{sub}})^{\text{wt}} / (k^{\text{ox}}/k^{\text{sub}})^{\text{mut}} \quad (7)$$

and the substituted position would always be expected to give rise to a negative coupling energy term ( $\Delta G_c < 0$ ). This follows because removal of the directly interacting enzyme side chain should reduce the substitution effect (i.e.  $\Delta\Delta G^{\text{sub}} \rightarrow$  zero because the mutant enzyme cannot “feel” the identity of the substituent anymore), thus making  $\Delta\Delta G^{\text{sub+mut}}$  smaller than the sum  $\Delta\Delta G^{\text{mut}} + \Delta\Delta G^{\text{sub}}$ . For a noninteracting side chain, its removal should have no effect on the interaction of the nonbridging substituent. Thus, the substituent effect would be unchanged as compared to the case of the wild-type enzyme, and the coupling energy would be zero (i.e.,  $\Delta\Delta G^{\text{sub+mut}} = \Delta\Delta G^{\text{mut}} + \Delta\Delta G^{\text{sub}}$ ). Finally, if a distant residue is mutated that indirectly upsets the direct interaction of the enzyme with the substituent group, making it either stronger or weaker, a positive or negative coupling energy will also result. Although this outcome has the potential of providing misleading information as to whether a side chain makes direct or indirect contact with a substituent, additional experiments and/or structural information can turn this ambiguity into a mechanistically informative result reflecting the cooperative nature of the interactions. These various

informative outcomes are discussed in the context of the individual enzyme systems explored below.

## 5. Experimental Techniques

### 5.1. Modified Substrates and Ligands

It is beyond the scope of this review to comprehensively cover the various methods for synthesis of phosphorothioate and methylphosphonate esters of phosphate. Accordingly, we refer the reader to key reviews in this area which serve as useful springboards to the primary synthetic literature. In general, both enzymatic and chemical synthetic methods abound. A key consideration in most protocols is the necessity to synthesize stereochemically pure compounds or, alternatively, be able to resolve them chromatographically. Reviews by Eckstein<sup>49</sup> and Frey<sup>6</sup> provide a comprehensive overview of the chemical and enzymatic methods for synthesis of phosphorothioate analogues of nucleotides, cyclic nucleotides, phospholipids, and several other phosphate esters of biological interest. The abbreviated discussion that follows extends the synthetic overview to the synthesis of phosphorothioate and methylphosphonate oligonucleotides.

Stereospecific incorporation of nonbridging sulfur substituents into the backbone of DNA or RNA has become fairly routine. Pure (*R<sub>p</sub>*) phosphorothioate linkages in DNA or RNA can be prepared enzymatically using pure nucleoside *S<sub>p</sub>*- $\alpha$ -thio triphosphates and a polymerase enzyme, where the reaction goes with inversion of configuration.<sup>50,51</sup> Chemical synthesis of racemic phosphorothioate linkages in oligonucleotides involves substituting the oxidation step of phosphoramidite based solid-phase synthesis with a sulfurization step using 3*H*-1,2-benzodithiol-3-one 1,1 dioxide.<sup>52</sup> This approach requires postsynthetic separation of the *R<sub>p</sub>* and *S<sub>p</sub>* diastereomers by C-18 reversed-phase HPLC, and configurational analysis of the product using enzymatic methods.<sup>53</sup> Although this separation usually works well for oligonucleotides shorter than about 20 nucleotide units, it may be problematic for certain nucleotide sequences or for longer oligonucleotides. An alternative approach that provides a stereochemically pure linkage for any length oligonucleotide is the block coupling of a diastereomerically pure dinucleoside phosphorothioate 3'-phosphoramidite precursor during solid-phase oligonucleotide synthesis.<sup>54</sup>

Incorporation of a 5'-bridging sulfur substituent in an oligonucleotide context was originally reported by Mag et al.,<sup>55</sup> and a modified procedure was subsequently reported by Burgin.<sup>56,57</sup> Both procedures involve preparation of a 5'-(*S*-trityl)-mercapto-5'-deoxynucleoside-3'-*O*-(2-cyanoethyl-*N,N*-diisopropyl) phosphoramidite which is used directly in solid-phase oligonucleotide synthesis with conventional nucleoside phosphoramidites. This synthesis requires careful purification of the full length oligonucleotide product because extension from the site of sulfur incorporation proceeds in much poorer yield than standard phosphoramidites.<sup>58</sup>

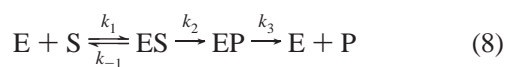
Several methods have been reported for the solid-phase synthesis and purification of stereoisomerically pure methylphosphonate oligonucleotides. Methods are similar to the general approaches described above for phosphorothioates, including the chromatographic separation of the diastereomers,<sup>59</sup> block coupling of diastereomerically pure dinucleoside methylphosphonates,<sup>60,61</sup> and kinetic resolution based on phosphorus III chemistry.<sup>62</sup>



## 5.2. Key Considerations in Binding and Kinetic Measurements

The first consideration when performing a mutational or chemical substitution measurement is the accuracy and precision of the binding or kinetic measurements and the actual magnitude of the measured effect. Because mutational and substitution effects are based on ratios of rate constants or equilibrium constants, the relative error in the ratio is determined by the square root of the sums of the squares of the relative errors in each kinetic or thermodynamic constant. Thus, measurement errors are magnified in the ratio. Compounding with the intrinsic measurement error is the enormous range of values for mutational and chemical substitution effects. For instance, effects of methyl or sulfur substitution as small as unity and as large as 100 000-fold have been measured (see examples that follow). Obviously, a crude assay with fairly large errors can provide useful results if the effect is on the high side of this range, but very good continuous kinetic assays or robust binding measurements are needed to measure effects in the range 2- to 10-fold.

Rigorous interpretation of mutational and thio effects also requires consideration of the rate-limiting steps of the steady-state reaction (eqs 8–10). For instance, if product release



$$k_{\text{cat}} = k_2 k_3 / (k_2 + k_3) \quad (9)$$

$$k_{\text{cat}}/K_m = k_1 k_2 / (k_{-1} + k_2) \quad (10)$$

( $k_3$ ) is severely rate-limiting for  $k_{\text{cat}}$  measurements with the oxygen substrate or with the wild-type enzyme, but the chemical step ( $k_2$ ) is rate-limiting for the substituted substrate or mutant enzyme, then the measured mutational or substitution effect will be significantly attenuated due to a change in rate-limiting step upon substitution or mutagenesis. This assertion assumes that the largest effect is on the chemical step (which is often true) and that the product release step has a smaller or nonexistent mutational or substitution effect. Under these conditions, it may be helpful to measure the effects on  $k_{\text{cat}}/K_m$  because this constant is unaffected by the product release step ( $k_3$ ) and only reports on the kinetic steps between substrate binding ( $k_1$ ) and the first irreversible step of the enzymatic reaction.<sup>63</sup> In many cases, the first irreversible step involves the chemical step ( $k_2$ ), allowing measurement of the full mutational or substitution effect on this kinetic constant. It must be kept in mind, however, that the full effect on the chemical step using  $k_{\text{cat}}/K_m$  conditions will only be realized when  $k_{-1} \gg k_2$ . This is identical to the essential requirement for measuring full (intrinsic) kinetic isotope effects, termed a small forward commitment to catalysis by Cleland.<sup>64</sup> A different approach that is frequently used is to employ an alternative substrate that is less reactive than the normal substrate, thus making the chemical step fully rate limiting. Alternatively, the mutational or substitution effect can be measured using single turnover conditions (i.e. where  $[E] \gg [S]$ ). Once again, under these conditions, product release is not part of the overall rate expression (i.e.  $k_{\text{obsd}} = k_2$ ), and very often, the full mutational or substitution effect on the chemical step is realized using such conditions. However, it should be pointed out that if the rate-limiting step involves a conformational step preceding the chemical step, the effects will still be masked using single turnover

conditions. The bottom line is this: detailed knowledge of the reaction mechanism and rate-limiting steps is critical for any study involving quantitative mutagenesis or chemical substitution measurements.

## 6. Examples Using Chemical Modification of Phosphate Esters Alone

Before introducing enzyme examples where mutagenesis and chemical substitution have been used in combination, it is informative to survey some representative studies where phosphorothioate and methylphosphonate substitution have been used in isolation. The purpose here is to gain a feeling for the magnitude of the effects in several different systems and see some of the limitations that can be ameliorated by combining substitution with mutagenesis. The thio effects and methyl effects for all of the systems discussed in sections 6 and 7 are compiled in Tables 1 and 2, respectively.

### 6.1. Protein–RNA Binding Reactions

Uhlenbeck and colleagues have performed a very comprehensive study of the effects of phosphorothioate and methylphosphonate substitution on the binding interaction of MS2 coat protein with a small RNA hairpin.<sup>65,66</sup> In this work, a single phosphorothioate or methylphosphonate linkage was introduced at 13 different positions in the RNA, providing a substantial database of measured effects. The value of this study was greatly increased because a high-resolution crystal structure was also available for the complex,<sup>67</sup> which allowed direct comparison of the substitution effects with structural data, as summarized in Figure 8 for the phosphorothioate substitutions. Generally speaking, there was an excellent correlation between the structure and modification data. At all of the eight phosphates where a contact was observed in the structure, at least one of the two sulfur diastereomers showed a binding effect, and at the four positions where no contact was observed, the binding was unchanged by sulfur substitution. Therefore, based on these findings, phosphorothioate substitution appears to be a reliable method for identifying protein–RNA backbone contacts.

In this study, the energetic effect of a single phosphorothioate substitution was in the range 0.4–1 kcal/mol, reflecting modest 2- to 5-fold changes in binding affinity. A key observation was that there was no apparent difference in the thio effect when the interacting group was a hydrogen bond donor or an ionic contact. Surprisingly, substitution at many positions gave rise to an increase in binding affinity for one isomer, while the other isomer showed either no change or a similar change in the same or opposite direction. Many of these diverse effects were rationalized by invoking steric effects, hydrophobic (solvation) effects, or differences in the charge or bond length of P–S relative to P–O bonds (see section 2). The authors also suggested that when a complex series of hydrogen bonds is formed between the protein and the RNA backbone, it is not possible to rationalize the substitution data based on the observed structural interactions. Thus, substitution of nonbridging atoms that form simple hydrogen bonds or ionic interactions with the protein generally gives rise to energetic effects that are most easily reconciled with structural information.

Methylphosphonate substitution in the same system resulted in even better agreement with the structural observations (Figure 9).<sup>65</sup> All phosphates that were in proximity to

**Table 1. Combined Energetic Effects of Enzyme Mutagenesis and Substrate Thio Substitution at Nonbridging Phosphoester Oxygens (kcal/mol)**

system	$\Delta\Delta G^{\text{bind } a}$	$\Delta G_c^{\text{bind } b}$	$\Delta\Delta G^{\text{chem}}$	$\Delta G_c^{\text{chem}}$	ref	system	$\Delta\Delta G^{\text{chem}}$	$\Delta G_c^{\text{chem}}$	ref
<i>RNA-Protein</i>					66	<i>UDG</i>			126
$R_p$	-0.7 to 1.0					WT			
$S_p$	-0.5 to 0.7					+1 $R_p$	-1.3		
<i>EcoRI</i>					54, 70	+1 $S_p$	-2.5		
clamp						-1 $R_p$	-0.6		
$R_p$	-0.7		-0.1			-1 $S_p$	-0.7		
$S_p$	-0.9		-0.7			-2 $R_p$	-2.1		
central						-2 $S_p$	+0.5		
$R_p$	+0.3		-0.4			S88A			
$S_p$	-1.7		+0.2			+1 $R_p$	-1.7	+0.4	
<i>EcoRV</i>					72	+1 $S_p$	-0.5	-2.0	
$R_p$	0.5 to 6.1					-1 $R_p$	-1.6	+1.0	
$S_p$	1.3 to 10					-1 $S_p$	-1.8	+1.1	
<i>vTopo</i>					84, 102	S189A			
WT						+1 $R_p$	-1.2	-0.1	
$R_p$	-1.7		-3.7			+1 $S_p$	-0.8	-1.7	
$S_p$	-0.6		-2.6			-1 $R_p$	-0.4	-0.1	
R130A						-1 $S_p$	-0.6	-0.1	
$R_p$	-1.4	-0.3	-1.3	<b>-2.4</b>		<i>Phospholipase-C</i>			131-134
$S_p$	0	-0.6	+0.3	<b>-2.9</b>		WT			
R130K						$R_p$	-2.2		
$R_p$	-1.3	-0.4	-1.4	<b>-2.3</b>		$S_p$	-7.5		
$S_p$	-1.0	+0.4	0	<b>-2.6</b>		D33N			
K167A						$R_p$	-1.0	-1.2	
$R_p$	-0.7	-1.0	-3.1	-0.6		$S_p$	-3.0	<b>-4.5</b>	
$S_p$	+0.4	-1.0	-3.0	+0.4		D33A			
R223A						$R_p$	-2.7	+0.5	
$R_p$	-1.4	-0.3	-1.6	<b>-2.1</b>		$S_p$	-3.7	<b>-3.8</b>	
$S_p$	0	-0.6	-1.9	-0.7		R69K			
H265A						$R_p$	-2.1	-0.1	
$R_p$			-2.1	<b>-1.6</b>		$S_p$	-2.0	<b>-5.5</b>	
$S_p$			-2.8	+0.2		<i>Protein Tyrosine Phosphatase</i>			44
<i>RNAse TI</i>					79	WT			
WT						$P_s$	-5.0		
$R_p$			-6.7			W354A			
$S_p$			-0.2			$P_s$	-4.5	-0.5	
Y38F						D356A			
$R_p$			-6.2	-0.5		$P_s$	-5.4	+0.4	
$S_p$			+1.6	<b>-1.8</b>		R409K			
H40A						$P_s$	-3.2	<b>-1.8</b>	
$R_p$						Q446A			
$S_p$			-1.0	+0.8		$P_s$	-3.8	<b>-1.2</b>	
E58A						Q450A			
$R_p$			-0.8	<b>-5.9</b>		$P_s$	-2.7	<b>-2.3</b>	
$S_p$			-1.0	+0.8					
H92Q									
$R_p$									
$S_p$			-0.9	+0.7					
F100A									
$R_p$			-3.0	<b>-3.7</b>					
$S_p$			-0.9	+0.7					

<sup>a</sup> The corresponding free energy changes for the substitution effects were calculated using  $\Delta\Delta G^{\text{bind}} = -RT \ln(K_D^{\text{ox}}/K_D^{\text{S}})$  and  $\Delta\Delta G^{\text{chem}} = -RT \ln(k^{\text{ox}}/k^{\text{S}})$  for the binding and chemical steps, respectively ( $T = 25^\circ$ ). <sup>b</sup> In the examples where both enzyme mutagenesis and phosphorothioate modifications were performed, the coupling energies for the interaction of an enzyme side chain with a nonbridging oxygen were determined using the following equations:  $\Delta G_c^{\text{bind}} = \Delta\Delta G_{\text{wt}}^{\text{bind}} - \Delta\Delta G_{\text{mut}}^{\text{bind}}$  and  $\Delta G_c^{\text{chem}} = \Delta\Delta G_{\text{wt}}^{\text{chem}} - \Delta\Delta G_{\text{mut}}^{\text{chem}}$ . A negative coupling energy is expected for a direct interaction with an enzyme side chain and a nonbridging oxygen. The coupling energies that correspond to a direct interaction between a nonbridging oxygen and an enzyme side chain, as judged by X-ray crystallography, are shown in bold in the table.

the protein showed a weaker binding affinity when substituted with a methylphosphonate linkage, and control positions showed no change. In two positions, a methylphosphonate isomer altered the binding affinity where no interaction was observed in the crystal structure, which was attributed to changes in the flexibility of the hairpin arising from the substitution. The authors concluded that methylphosphonate substitution was superior to phosphorothioate substitution because it nearly always decreases the binding affinity, whereas phosphorothioate substitution either strengthened or weakened binding interactions in unpredictable ways (see

above). A useful advantage of the methylphosphonate effects was that they were typically much larger than the sulfur substitution effects, falling in the range 2- to 500-fold. In addition, it was noted that the effects were not stereospecific for five out of seven linkages that were in direct contact with the enzyme. This is consistent with the expectation that removal of the methyl group removes a hydrogen bond acceptor and also abolishes the negative charge of the remaining nonbridging oxygen, negating favorable interactions at both positions. In conclusion, these studies largely validate the utility of both phosphorothioate and methylphos-

**Table 2. Combined Energetic Effects (kcal/mol) of Enzyme Mutagenesis and Substrate Methyl Substitution of Nonbridging Phosphoester Oxygens**

system	$\Delta\Delta G^{\text{bind } a}$	$\Delta\Delta G^{\text{chem}}$	$\Delta G_c^{\text{chem } b}$	ref	system	$\Delta\Delta G^{\text{bind}}$	$\Delta\Delta G^{\text{chem}}$	ref
<i>RNA-Protein</i>				65	<i>UDG</i>			125
$R_p$	-0.7 to 3.4				WT/substrate <sup>c</sup>			
$S_p$	-0.4 to 2.3				+2 fast		-0.4	
					+2 slow		-0.4	
<i>vTopo</i>				104, 105	+1 fast		+3.6	
WT					+1 slow		+2.3	
$R_p$		-4.8			-1 fast		+5.0	
$S_p$		-3.2			-1 slow		+1.5	
R223A					-2 fast		+4.5	
$R_p$		+0.1	-4.9		-2 slow		+4.8	
$S_p$		+3.1	-6.3		WT/TS analogue <sup>d</sup>			
R223K					+1 fast	+6.3		
$R_p$		-4.9	+0.1		+1 slow	+6.3		
$S_p$		-2.0	-1.2		-1 fast	+5.8		
H265A					-1 slow	+3.0		
$R_p$		-4.7	-0.1		-2 fast	+7.2		
$S_p$		+0.1	-3.3		-2 slow	+7.3		

<sup>a</sup> The corresponding free energy changes for the substitution effects were then calculated using  $\Delta\Delta G^{\text{bind}} = -RT \ln(K_D^{\text{ox}}/K_D^{\text{Me}})$  and  $\Delta\Delta G^{\text{chem}} = -RT \ln(k^{\text{ox}}/k^{\text{Me}})$  ( $T = 25^\circ$ ). The  $R_p$  and  $S_p$  designations refer to the respective stereoisomers created at the substitution site upon methyl modification.

<sup>b</sup> In the topoisomerase example, the coupling energies for the interaction of an enzyme side chain with a nonbridging oxygen were determined using the following equations:  $\Delta G_c^{\text{bind}} = \Delta\Delta G_{\text{wt}}^{\text{bind}} - \Delta\Delta G_{\text{mut}}^{\text{bind}}$  and  $\Delta G_c^{\text{chem}} = \Delta\Delta G_{\text{wt}}^{\text{chem}} - \Delta\Delta G_{\text{mut}}^{\text{chem}}$ . <sup>c</sup> In the UDG system, the designations fast and slow correspond to the faster and slower migrating diastereomers during HPLC elution of the methylphosphonate substituted substrate. See Figure 22 for the numbering key. <sup>d</sup> The cationic transition-state (TS) analogue corresponds to the 1-azadeoxyribose oxacarbenium ion mimic (see Figures 20 and 22).

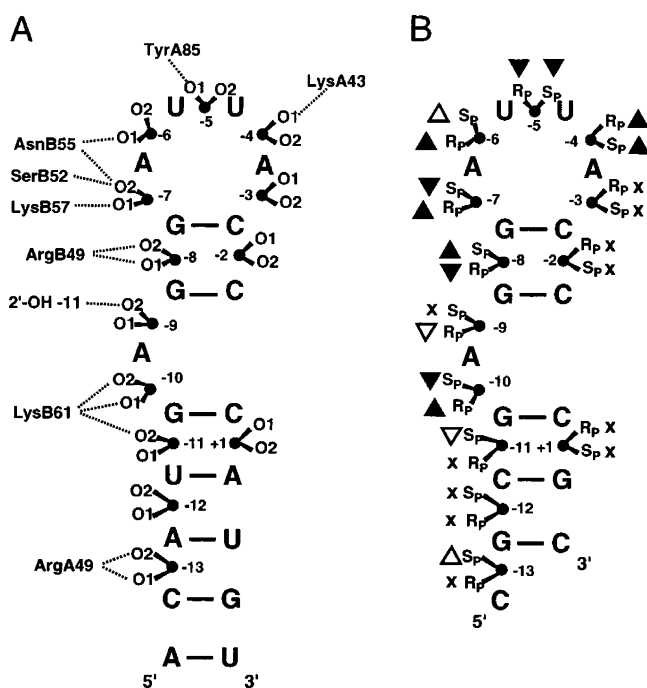


**Figure 8.** Interactions between MS2 coat protein and RNA.<sup>56</sup> (A) Representation of the protein-phosphate contacts observed in the crystal structure of the complex of MS2 coat protein bound to a 21-nucleotide RNA hairpin. The prefixes A and B specify the amino acids in the two monomers of the dimeric coat protein. O1 and O2 correspond to the  $R_p$  and  $S_p$  phosphorothioate diastereomers. (B) Thio effects on binding. Black triangles indicate the positions with the largest thio effects of binding; upward and downward pointing triangles indicate stronger and weaker binding for the phosphorothioate RNA, respectively. Small effects are indicated by white triangles, and sites where binding was unaffected by substitution are marked with an x.

phosphate substitution for identifying important binding contacts, but as will be detailed below, the combined mutagenesis and substitution methodology increases the information content of the substitution effects.

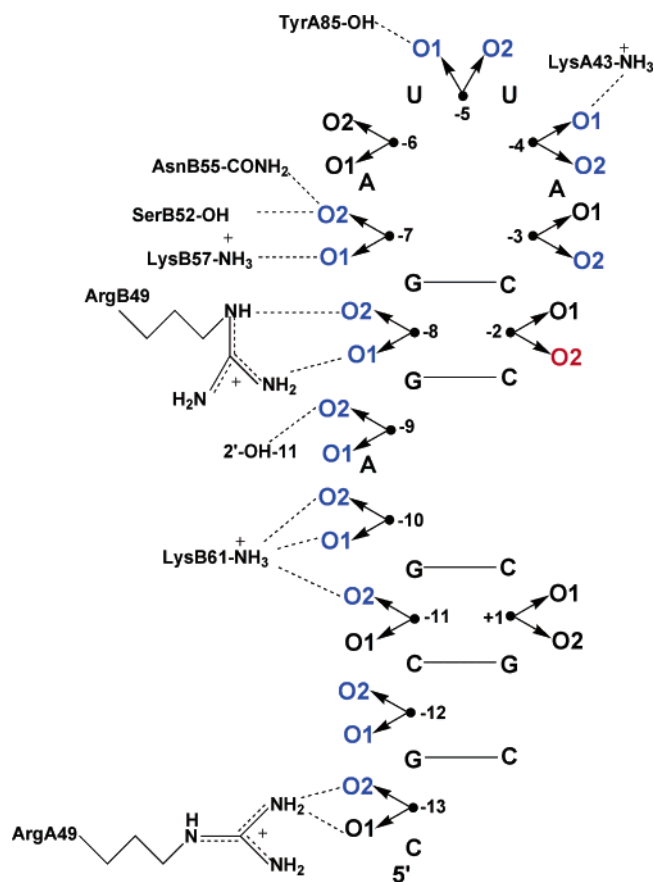


**Figure 9.** Changes in MS2 protein-RNA binding affinity arising from methylphosphonate substitution.<sup>57</sup> Oxygens where substitution strengthens, weakens, or has no effect on binding are shown in red, blue, and black, respectively.

## 6.2. Reactions with DNA: *EcoRI* and *EcoRV* Restriction Enzymes

Phosphorothioate and methylphosphonate substituted DNA have been used extensively to study the site-specific DNA

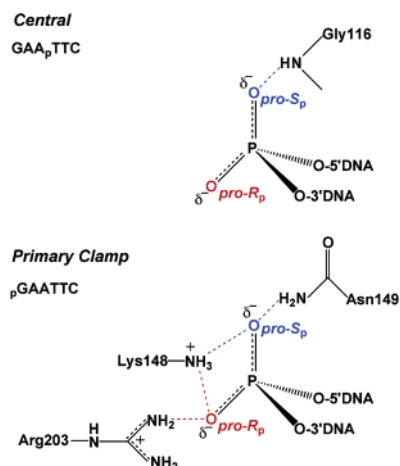


**Figure 10.** Interactions of *EcoRI* with the central and primary clamp phosphates as observed in the crystal structure 1ERI.

binding and phosphodiester hydrolysis reactions of several DNA restriction endonucleases. The approach was first explored by Eckstein and colleagues,<sup>68,69</sup> and it was later applied by others to the prototypic restriction endonucleases *EcoRI* and *EcoRV*.<sup>53,54,70</sup>

Jen-Jacobson and co-workers probed the ground-state binding contacts between *EcoRI* and the central phosphate (**p**) of its recognition sequence G $\downarrow$ AApTTC as well as the “primary clamp” phosphate pG $\downarrow$ AATTC using stereospecific phosphorothioate linkages (the arrows mark the phosphodiester linkage that is cleaved during the hydrolysis reaction).<sup>54,70</sup> These studies were strengthened by the availability of a crystal structure of the protein–DNA complex which showed that these two phosphates have very different interactions with the enzyme<sup>71</sup> (pdb code 1ERI) (Figure 10). The *pro-S<sub>p</sub>* oxygen of the central phosphate accepts a hydrogen bond from the backbone NH of a glycine residue (N  $\rightarrow$  O distance of 2.9 Å), but the other oxygen of this linkage does not interact with the protein at all. An entirely different arrangement prevails for the primary clamp phosphate, which was found to be completely engulfed by protein interactions. The *pro-R<sub>p</sub>* oxygen of this phosphate is directed toward the major groove and contacts the guanidino group of Arg203 and the side chain amino group of Lys148. The *pro-S<sub>p</sub>* oxygen receives hydrogen bonds from the side chain of Asn149 and the main chain amide of Lys89. In addition, these primary contact residues are connected via hydrogen bonds to other residues that contact the DNA backbone and bases or other enzyme residues involved directly in catalysis. The very different interactions of the enzyme with these two linkages make an interesting case study in the interpretation of thio effects, as detailed below.

As observed with the MS2 coat protein–RNA complex, both increases and decreases in ground-state binding affinity in the range  $-0.7$  to  $+1.0$  kcal/mol were observed upon sulfur substitution at these two linkages of the *EcoRI* site. Substitution at the noninteracting *S<sub>p</sub>* position of the central phosphate gave rise to 20-fold tighter binding, while the interacting *R<sub>p</sub>* substitution led to 2-fold weaker binding. This unanticipated effect was rationalized by the proposal that *S<sub>p</sub>* sulfur substitution increased the P–O bond order of the remaining P–O bond, thereby shortening it, increasing the hydrogen bond distance by 0.06 Å, and resulting in a more favorable hydrogen bond distance of  $\sim 2.8$  Å between the *R<sub>p</sub>* oxygen and the glycine NH. Accordingly, the weaker binding observed upon substitution of the *pro-R<sub>p</sub>* oxygen with

sulfur was attributed to steric conflicts arising from the longer P–S bond (an increase of 0.6 Å over the P–O bond).<sup>6,15</sup> However, these explanations are somewhat unsatisfying. It is not clear why a small 0.06 Å decrease in hydrogen bond distance and, in addition, ablation of negative charge would give rise to a substantial 20-fold increase in affinity. Moreover, a 0.6 Å increase in P–S bond length with the *R<sub>p</sub>* substituent would be expected to severely disrupt hydrogen bonding, yet only a small 2-fold damaging effect is observed. Outcomes such as this may benefit from additional mutagenesis experiments, or perhaps measurements of methylphosphonate effects, to provide a more sound understanding of the interactions.

The *R<sub>p</sub>* and *S<sub>p</sub>* substitutions at the primary clamp phosphate linkage of the *EcoRI* recognition sequence gave rise to similar 3- and 5-fold decreases in binding affinity as seen for the *R<sub>p</sub>*-position of the central phosphate. This was surprising because the central and primary clamp phosphate groups make completely different contacts with the protein (see above). The small magnitude of these effects makes them difficult to interpret in terms of structure, but the authors suggested that the effects arose from a combination of changes in charge and bond orders at the substituted position, which in turn led to disruption of the other interaction due to the intimate coupling to the recognition interface.

Thio effects on the chemical step in *EcoRI* catalysis were measured by substituting the central and primary clamp phosphate oxygens.<sup>54,70</sup> These measurements, which were performed under single turnover conditions, represent indirect effects on the activation barrier, because the central and primary clamp phosphates are not the sites of cleavage by *EcoRI*. With both substituted phosphates, one isomer showed no effect and the other produced a small 2- to 3-fold rate decrease. The generally small or absent thio effect on the activation barrier and the observed ground-state stabilization of as much as 1.7 kcal/mol with some substitutions indicate that thio substitution has approximately equal energetic effects in the ground state and transition state in this system. In general, the small thio effects and complex interaction network of *EcoRI* recognition make definitive conclusions about these interactions quite tenuous.

Connolly and co-workers synthesized a set of DNA dodecameric oligonucleotides containing the recognition sequence for *EcoRV* restriction endonuclease and introduced stereospecific phosphorothioate linkages at the central nine positions, including the scissile linkage.<sup>72</sup> The thio effect results were then compared with the crystal structure of the enzyme–DNA complex.<sup>73</sup> The important phosphates, as assessed by thio effect measurements, comprised GACG**p**<sup>4</sup>-Ap<sup>5</sup>Tp<sup>6</sup> $\downarrow$ Ap<sup>7</sup>Tp<sup>8</sup>Cp<sup>9</sup>GTC of the dodecamer. Substitution at phosphate linkages **p**<sup>4</sup>, **p**<sup>5</sup>, **p**<sup>8</sup>, and **p**<sup>9</sup> produced 5- to 30-fold decreases in  $k_{\text{cat}}$  and, in general, 1.5- to 10-fold lower  $K_{\text{m}}$  values. Much greater deleterious effects were observed at the scissile phosphate **p**<sup>6</sup> and the adjacent phosphate **p**<sup>7</sup>: both phosphorothioate isomers at the scissile position were so damaging that rate measurements were precluded, and *S<sub>p</sub>* substitution at **p**<sup>7</sup> also abolished catalysis, while *R<sub>p</sub>* substitution had no effect. In the case of the scissile phosphate, the effects were attributed to cooperative disruption of a network of interactions for the *R<sub>p</sub>* isomer, and in the case of the *S<sub>p</sub>* isomer, they were attributed to reduced Mg<sup>2+</sup> binding. The disruption of metal binding was supported by crystallographic studies which show that the *pro-S<sub>p</sub>* oxygen is one of the ligands to the catalytic Mg<sup>2+</sup>. Thus, the observed structural



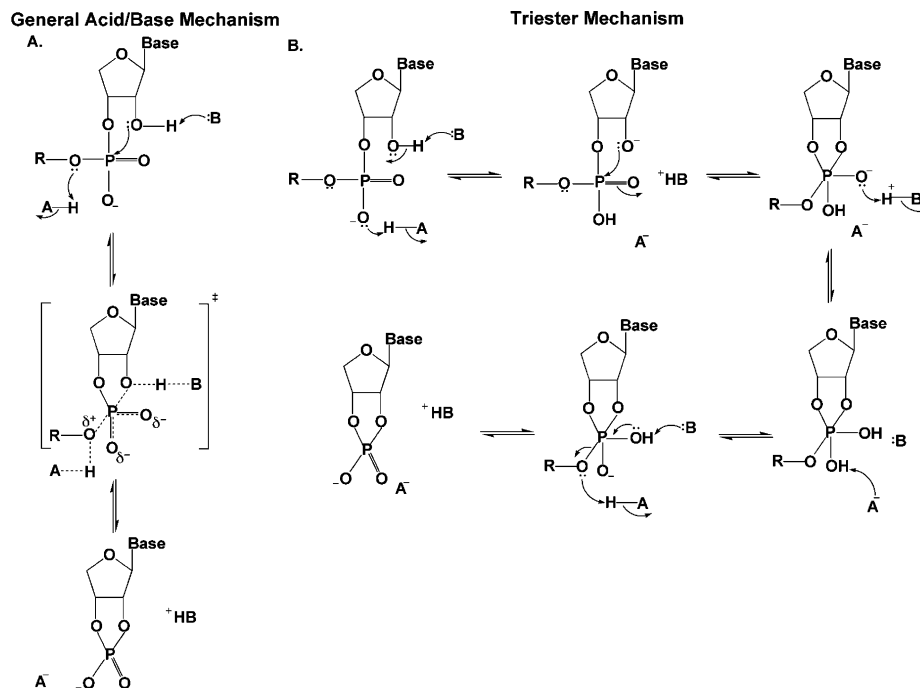


**Figure 11.** Proposed mechanisms for RNase T1 catalysis: (A) general acid–base mechanism;<sup>66</sup> (B) triester mechanism.<sup>67</sup>

interactions provide convincing support for the interpretation of the large  $S_p$  thio effects because sulfur is a poor ligand for hard metals such as  $Mg^{2+}$ .<sup>12</sup> For the  $p^7$  phosphate, the low activity of the  $S_p$  phosphorothioate substituted substrate was attributed to a role for the *pro-R\_p* oxygen of the  $p^7$  phosphate as a general base to deprotonate the catalytic water. The profound activity decrease is thus brought about by localization of the negative charge on the  $S_p$  sulfur and by the increased double bond character of the remaining  $R_p$  oxygen, which significantly lowers its  $pK_a$  such that it cannot serve as an efficient general base. This interpretation was supported by methylphosphonate substitution at the same phosphate linkage of 17 different restriction enzymes,<sup>74</sup> where only five enzymes were found not to be significantly inhibited by this substitution. Although these findings suggest a role for the *pro-R\_p* oxygen as a general base, it is not clear how a nonbridging phosphodiester oxygen with a  $pK_a \sim 1.5$  in water could serve as an efficient general base unless the enzyme environment is highly desolvated or a local negative potential is increasing its basicity.

## 7. Examples Combining Chemical Modification and Mutagenesis

### 7.1. RNase T<sub>1</sub>

Despite extensive research, the detailed series of chemical events in ribonuclease (RNase) catalyzed phosphoryl transfers are still debated.<sup>75–78</sup> Enzymes such as RNase A and RNase T<sub>1</sub> cleave phosphodiester bonds in RNA using the 2'-OH of the RNA as the initial nucleophile to form a 2',3' cyclic phosphodiester intermediate that is subsequently hydrolyzed (Figure 11). Two general mechanisms for formation of the cyclic phosphate intermediate have been proposed. The first involves concerted general-acid base catalysis by two conserved histidine residues: the base deprotonates the 2'-OH, and the acid protonates the 5'-OH leaving group (Figure 11A). The second type of mechanism is distinguished by initial proton transfer to a nonbridging oxygen, which is

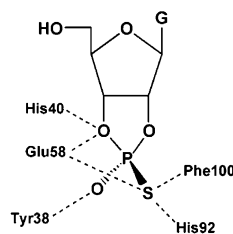


**Figure 12.** Active site interactions of RNase T1 with *exo*-( $S_p$ )-2',3'-cGMP(S), the product of transphosphorylation of ( $S_p$ )-Gp(S)U.

then followed by 2'-OH attack. In the second mechanism, preequilibrium protonation of the nonbridging oxygen makes the second nucleophilic addition step triester-like (Figure 11B). For RNase A, small nonbridging thio effects have been interpreted in favor of the concerted acid–base mechanism,<sup>75</sup> because nucleophilic substitution at phosphate triesters is expected to have a thio effect of around 100 (Figure 6).

#### 7.1.1. Nonbridging Phosphorothioate Substitution and RNase T<sub>1</sub> Mutagenesis

Steyaert and colleagues have investigated the nonbridging thio effects for RNase T1 and, in conjunction with mutagenesis, concluded that, unlike RNase A, this enzyme uses a triester-like mechanism.<sup>79</sup> The active site of RNase T1, in complex with *exo* ( $S_p$ ) 2',3'-cGMP(S), which is the product of the transphosphorylation of  $S_p$  Gp(S)U, is shown in Figure 12. The structure suggests close proximity of the aromatic ring of Phe100 and the side chain of Glu58 to the  $S_p$  sulfur but not to the  $R_p$  oxygen. In addition, both His40 and Glu58 are within hydrogen bonding distance of the 2'-oxygen of the cyclic phosphate intermediate, indicating that His40 would be the general base if a concerted general acid–base mechanism is followed as suggested for RNase A. Consistent with the structure, the authors found that  $S_p$  Gp(S)U had an enormous thio effect on  $k_{cat}/K_m$  of 88 500, whereas the  $R_p$  form showed a negligible effect of 1.5.<sup>80</sup> In addition, no thio effect on binding was observed, indicating that the perturbed interactions were in the transition state. The  $S_p$  thio effect

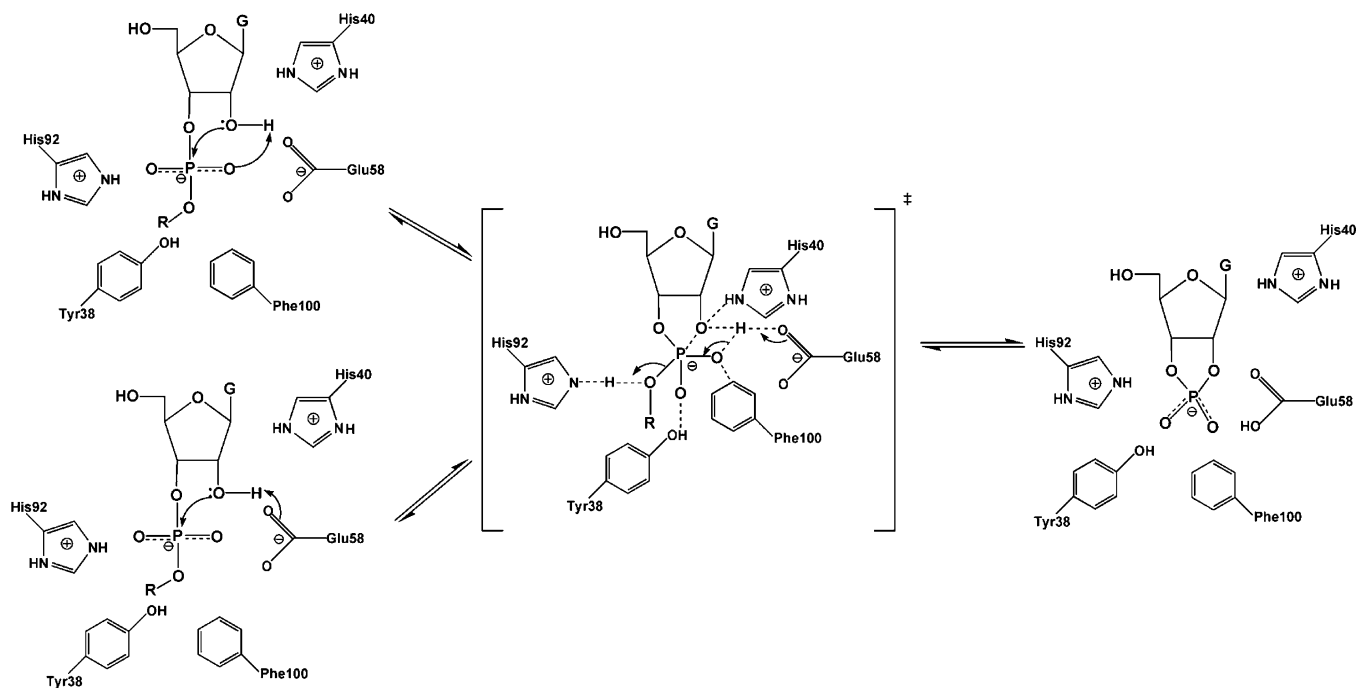


**Figure 13.** Putative triester-like transition state for formation of the cyclic intermediate in the RNase T<sub>1</sub> reaction involving a three-centered hydrogen bond with the pro-*S<sub>p</sub>* oxygen and Glu-58.<sup>70</sup>

on  $k_{\text{cat}}/K_m$  is one of the largest ever reported for a nonmetal assisted reaction, and it is only eclipsed by the  $S_p$  thio effect for phosphatidylinositol-specific phospholipase C, which, interestingly, proceeds by a similar cyclic phosphate mechanism (see section 7.4). The large thio effects in these two related systems suggest that  $S_p$  sulfur substitution has an unusually deleterious effect in the transition state for formation of cyclic phosphate intermediates. This could arise from highly specific electronic or geometric constraints of this transition state in the active sites of enzymes.

As anticipated, mutation of the residues that were thought to directly interact with the pro- $S_p$  oxygen of RNase T<sub>1</sub> (F100A and E58A) resulted in  $\sim 10^2$ - to  $10^4$ -fold decreases in the  $S_p$  thio effect, with the largest reduction seen with E58A. Either mutation of other residues produced small changes in the thio effect or, for the H92Q and H40A mutations, the activity was too low to be detected with the  $S_p$  sulfur substrate. (A lower limit thio effect of  $>330$  for both histidine mutants can be estimated from the detection limits of the assay.) The diminished thio effect for E58A corresponded to a coupling energy of  $-5.9$  kcal/mol (Table 1). Based on the large thio effects and the mutagenesis results, these authors proposed a triester-like transition state for formation of the cyclic intermediate involving a three-centered hydrogen bond with the pro- $S_p$  oxygen and Glu-58 (Figure 13). The authors argued that the lower proton affinity of sulfur impaired proton transfer. However, alternative explanations such as stereospecific steric effects on catalysis are not excluded. Furthermore, the similarly large  $S_p$  thio effect for cyclic phosphate formation with phosphatidylinositol-specific phospholipase C (section 7.4) was reconciled with a simple general acid–base mechanism without invoking protonation to form a triester-like transition state. One lesson of enzymatic thio effects is that it is virtually impossible to use thio effects alone to define transition-state structure because of unknown steric and electronic requirements in the transition state that overwhelm the simple trends from solution reactions (Figure 6).

## 7.2. Vaccinia DNA Topoisomerase I (vTopo)

The vaccinia virus type IB DNA topoisomerase (vTopo) is a well-studied enzyme where both phosphorothioate and methylphosphonate chemical modifications of the DNA backbone have been combined with enzyme mutagenesis to reveal a detailed interaction map between the enzyme and the DNA substrate. The type IB topoisomerase reaction is freely reversible and occurs by four discrete steps (Figure 14). These steps involve (i) noncovalent binding of the enzyme to the DNA with a dissociation constant  $K_D$ , (ii) cleavage of a single DNA strand leading to formation of a covalent 3'-phosphotyrosine linkage and a free 5'-hydroxyl leaving group ( $k_{\text{cl}}$ ), (iii) release of superhelical tension by a strand rotation mechanism ( $k_{\text{sup}}$ ), and (iv) religation of the DNA break by attack of the 5'-hydroxyl nucleophile ( $k_r$ ). The vTopo enzyme is unique in that it shows high specificity for cleavage at the pentapyrimidine recognition sequence 5'-(C/T)<sup>+5</sup>C<sup>4+</sup>C<sup>3+</sup>T<sup>+2</sup>T<sup>+1</sup>pN<sup>-1</sup> (the arrow indicates the site of covalent attachment). The binding, cleavage, and religation events are most easily studied using synthetic oligonucleotide DNA substrates of length 18–40 base pairs, and rigorous methods have been developed to measure each step of the vTopo reaction.<sup>58,81–85</sup> Alanine scanning of about 142 amino acids in vTopo has been performed to identify essential catalytic residues.<sup>86</sup> From this study, only seven amino acids were found to decrease enzyme DNA cleavage activity by greater than 100-fold: Arg130 ( $10^5$ -fold), Gly132 ( $10^2$ -fold), Tyr136 ( $10^3$ -fold), Lys167 ( $10^5$ -fold), Arg223 ( $10^5$ -fold), His265 ( $10^5$ -fold), and Tyr274 ( $>10^5$ -fold) (the active site nucleophile). It is important to note that five of the six essential amino acids are strictly conserved in every member of the eukaryotic type IB enzyme family (the exception is Tyr136).<sup>87</sup>

Although the vTopo protein–DNA complex has been found to be refractory to crystallization, several X-ray structures of DNA bound to the highly homologous human topoisomerase IB have been solved, both in the noncovalent and phosphotyrosine covalent complexes.<sup>88–93</sup> These struc-

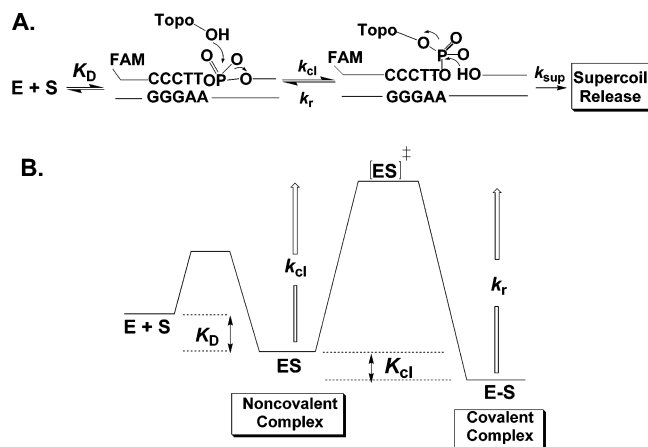


**Figure 14.** Topoisomerase reaction cycle. (A) The three steps in the vTopo reaction involve DNA binding, reversible DNA backbone cleavage described by the rate constants  $k_{cl}$  and  $k_r$ , and, for supercoiled DNA substrates, supercoil relaxation while the enzyme is covalently attached to the phosphodiester backbone ( $k_{sup}$ ). Relaxation occurs by a “free rotation” mechanism in which the noncovalently bound end swivels around the helix axis. The number of supercoils that are removed after a single cleavage event is dependent on the ratio  $k_{sup}/k_r$ : if  $k_r$  is rapid, there is no opportunity for DNA rotation before the strand is resealed. (B) Free energy reaction coordinate profile depicting the thermodynamic and kinetic barriers of the reaction. The rate constants and equilibrium constants refer to the free energy barriers defined by  $K = \exp(-\Delta G/RT)$  and  $k = (k_B T/h) \exp(-\Delta G^\ddagger/RT)$ .

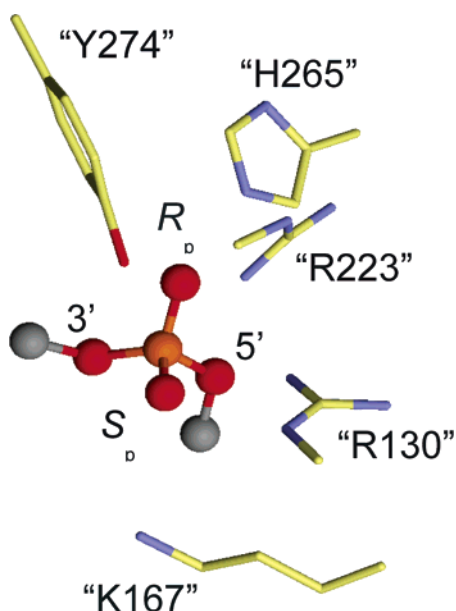


**Figure 15.** Interactions in the vTopo Michaelis complex with DNA. The interactions are from the crystal structure of the closely related human topoisomerase IB (pdb code 1EJ9), and the residue numbering corresponds to vTopo.

tures revealed that the amino acid equivalents of Arg130, Lys167, Arg223, and His265 of the vaccinia enzyme were near the scissile phosphate (Figure 15). From these structural studies, Arg130 was observed to contact both of the nonbridging oxygens, whereas Arg223 interacted only with *pro-R<sub>p</sub>* oxygen. However, the roles of His265 and Lys167 were ambiguous because they were either too far away from the scissile phosphate to assist catalysis (Lys167) or roughly equidistant from both the *pro-R<sub>p</sub>* nonbridging oxygen and the 5'-O leaving group (His265). Thus, these crystallographic efforts left key questions unresolved, including the exact roles

**Table 3. Bridging Thio Effects (TE<sup>B</sup>) on VTopo DNA Cleavage<sup>a</sup>**

enzyme	TE <sup>B</sup>
wt	0.7
H265A	1.8
R130A	190
R130K	2600
K167A	370
R130K:K167A	2000
R223A	0.8

<sup>a</sup> From refs 94 and 95. TE<sup>B</sup> (bridging thio effect) =  $k^{ox}/k^s$ .

of Lys167 and His265 and the identity of the general acid catalyst of leaving group expulsion. Thus, alternative approaches to obtain structural information for the various catalytic intermediates and transition states became quite important to increase the understanding of this enzyme reaction.

### 7.2.1. Bridging Phosphorothioate Substitution and VTopo Mutagenesis

To determine the identity of the general acid catalyst, Shuman and co-workers determined the activity effects of 5' bridging sulfur substitution at the scissile phosphate for the wild-type enzyme and several alanine mutants of the enzyme (Table 3).<sup>94,95</sup> The expectation was that mutation of the true general acid to alanine (i.e. a residue that does not possess a proton donor function) would significantly reduce the activity of topoisomerase toward the oxygen substrate but not the sulfur substrate. The activity rescue of the mutant enzyme by a 5'-bridging sulfur provides strong evidence that the mutated residue is the general acid functionality, because a 5' sulfur leaving group does not need assistance from a general acid because of its low pK<sub>a</sub> (see section 3). Thus, a “5'-S rescue” of much greater than unity (eq 11) provides a

$$5'\text{-S rescue} = (\text{TE}^{\text{mut}}/\text{TE}^{\text{wt}}) \quad (11)$$

strong indicator for the identity of the general acid catalyst. In this equation, TE<sup>mut</sup> and TE<sup>wt</sup> are defined as  $k^{ox}/k^s$  for the mutant and wild-type enzymes, respectively. In addition to P–S bridging linkages, it should be noted that P–N bridging linkages of phosphoamides can be either intrinsically less or more reactive than the corresponding P–O linkage depending on the relative pK<sub>a</sub> values for the leaving groups<sup>96–98</sup> and possible stereoelectronic differences between these reactions.<sup>99,100</sup> We are not aware of any studies of enzyme catalyzed reactions that have employed substrates with P–N linkages in combination with mutagenesis.

In this work, the R223A and H265A mutants showed little or no 5'-S rescue, indicating that neither of these residues were the general acid (Table 3). In contrast, the R130A and K167A enzymes exhibited large 5'-S rescues of 190 and 370, respectively. Interestingly, the R130K mutant showed the largest 5'-S rescue (2600-fold). To explain these observations, Shuman and co-workers suggested that Arg130 and Lys167 interacted with each other during the proton donation step, thereby forming a proton relay chain.<sup>95</sup> Thus, the direct proton donor to the 5'-oxygen remained elusive in these studies (i.e. R130 → K167 → 5'-O vs K167 → R130 → 5'-O). Of the two possibilities, Shuman et al. suggested that Lys167 was the direct proton donor, with Arg130 serving as indirect role. This tentative assignment was based on the fact that Lys167 was located within hydrogen bonding distance (3.2 Å) of the 5'-OH of the cleaved strand in the

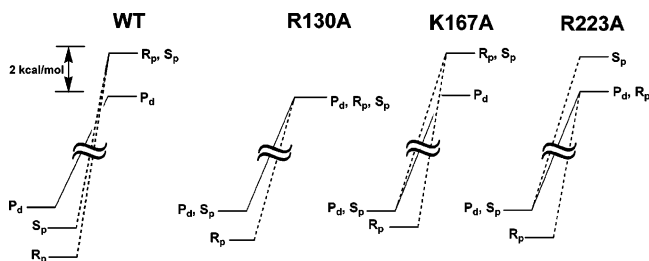


**Figure 16.** Energetic effects of thio substitution in the ground state and transition state for DNA cleavage by vTopo and three catalytic site mutants (see text).<sup>88</sup> P<sub>d</sub>, phosphodiester.

cocrystal structure of the related enzyme Flp recombinase.<sup>101</sup> In this mechanism where Lys167 is the direct proton donor, Arg130 was proposed to lower the pK<sub>a</sub> of Lys167 through an electrostatic mechanism. However, the choice of Lys167 as the direct proton donor does not explain the 10-fold larger rescue observed for the R130K mutant as compared to K167A or R130A. As described below, the nonbridging thio effect measurements of Nagarajan and Stivers suggested a plausible mechanism that accounts for all of these findings.

### 7.2.2. Dissecting the Energetics of Nonbridging Phosphorothioate Substitution with vTopo Mutants

Two comprehensive studies examined the effects of mutagenesis and nonbridging phosphorothioate substitution on the vTopo reaction.<sup>84,102</sup> A key aspect of this work was the measurement of both binding and kinetic effects for each substitution and mutant, providing the necessary energetic measurements to understand how enzyme interactions with the scissile phosphate changed between the ground state and transition state, as shown in Figure 16 for the wild-type, R130A, K167A, and R223A enzymes. In this analysis, the thio effects (TEs) on binding and cleavage were first converted into difference free energy changes using the simple thermodynamic equations below (eqs 12 and 13).

$$\Delta\Delta G_{\text{bind}} = -RT \ln \text{TE}^{\text{bind}} \quad (12)$$

$$\Delta\Delta G_{\text{cleavage}} = -RT \ln \text{TE}^{\text{cleavage}} \quad (13)$$

Thus, with independent measurements of the effects of sulfur substitution on binding and the activation barrier, it was possible to dissect the overall effect on the cleavage activation barrier into ground-state and transition-state contributions. For example, in wild-type vTopo, R<sub>p</sub> sulfur substitution led to an overall 3.6 kcal/mol increase in the cleavage activation barrier, which is comprised of 1.7 kcal/mol ground-state stabilization and a 1.9 kcal/mol destabilization in the transition state for cleavage (Figure 16). In contrast, the S<sub>p</sub> sulfur substituent had little effect on the ground-state binding but produced an identical 1.9 kcal/mol destabilization in the transition state. These findings suggested that the R<sub>p</sub> sulfur anion (but not the S<sub>p</sub>) interacts favorably in the ground state with a cluster of positively charged residues defining the active site. When the transition-state conformation is reached, an additional interaction with the S<sub>p</sub> position becomes important. These results suggested a pathway for forming the transition state that involved an initial loose organization of enzyme groups around the phosphodiester linkage in the ground-state involving long-range electrostatic attraction with the R<sub>p</sub> substituent (as indicated by the strong salt dependence of the thio effects). More extensive interactions with the phosphoryl group then

ensue as the transition-state conformation is reached. A summary of the salient measurements for each mutant and their interpretations follows.

**R130A(K).** Removal of Arg130 only slightly reduced the R<sub>p</sub> thio effect in the ground state as compared to the case of the wild-type enzyme, but it essentially abolished the interaction, giving rise to the R<sub>p</sub> and S<sub>p</sub> thio effect in the transition state (Figure 16). An additional interesting finding with R130A is that the R<sub>p</sub> thio effect on the cleavage activation barrier arises entirely from *ground-state stabilization*, whereas the wild-type enzyme shows both ground-state stabilization and transition-state destabilization effects (Figure 16). It would appear that removal of Arg130 disrupts all of enzyme interactions with the R<sub>p</sub> position in the transition state (including the interactions of His265 and Arg223). Such a scenario explains the especially large damaging effect of the R130A mutation. Since the R130K mutation has the same damaging effect on the cleavage rate as R130A and, in addition, produces similar nonbridging thio effects, then the Lys130 amino group must not interact with either of the nonbridging oxygens. This is a reasonable result, as the shorter lysine side chain is unable to extend out far enough to make these interactions.

**K167A.** Removal of Lys167 reduces the binding affinity of the enzyme to the S<sub>p</sub> and R<sub>p</sub> sulfurs in the ground state as compared to the wild-type enzyme (Figure 16), suggesting that Lys167 directly or indirectly affects electrostatic interactions with these positions. In the transition state, removal of Lys167 resulted in a 1.5 kcal/mol increase in the transition-state energy for the S<sub>p</sub> substrate compared to the wild-type enzyme (Figure 16). This result indicates that in the *absence* of Lys167 a stronger interaction with the *pro-S<sub>p</sub>* oxygen in the transition state exists. Since both structural and thio effect measurements indicate that Arg130 is the only residue that directly contacts the *pro-S<sub>p</sub>* oxygen, then a likely scenario is that the Arg130–*proS<sub>p</sub>* oxygen interaction is stronger when electrostatic repulsion by the nearby Lys167 is removed. This finding provided strong evidence for a thermodynamic linkage between Arg130 and Lys167 residues, as required for the proton relay mechanism proposed by Shuman and colleagues.<sup>95</sup>

**R223A.** Removal of Arg223 caused a decreased R<sub>p</sub> thio effect on ground-state binding and no change in the S<sub>p</sub> thio effect relative to the case of wild-type enzyme. The stereo-selective decrease in the R<sub>p</sub> thio effect on cleavage (relative to the case of the wild-type) indicated weaker ground-state and transition-state interactions with the R<sub>p</sub> sulfur in the absence of Arg223. The results indicated that the *pro-S<sub>p</sub>* oxygen did not interact with Arg223 (Figure 16).

**H265A.** Removal of His265 caused an 11-fold decrease in the R<sub>p</sub> thio effect on cleavage and a 3-fold increase in the S<sub>p</sub> thio effect.<sup>102</sup> These measurements support a favorable interaction of His265 with the *pro-R<sub>p</sub>* oxygen and an indirect, anticooperative interaction with the *pro-S<sub>p</sub>* oxygen.

### 7.2.3. Structural Interpretations

These mutational and nonbridging thio effect measurements allowed the construction of interaction maps for the nonbridging atoms in the ground state and pentacoordinate transition state for DNA cleavage (Figure 17). The interactions shown were inferred entirely from the thio effect measurements and are consistent with the positions of these groups in the crystal structure of the human enzyme shown in Figure 15.



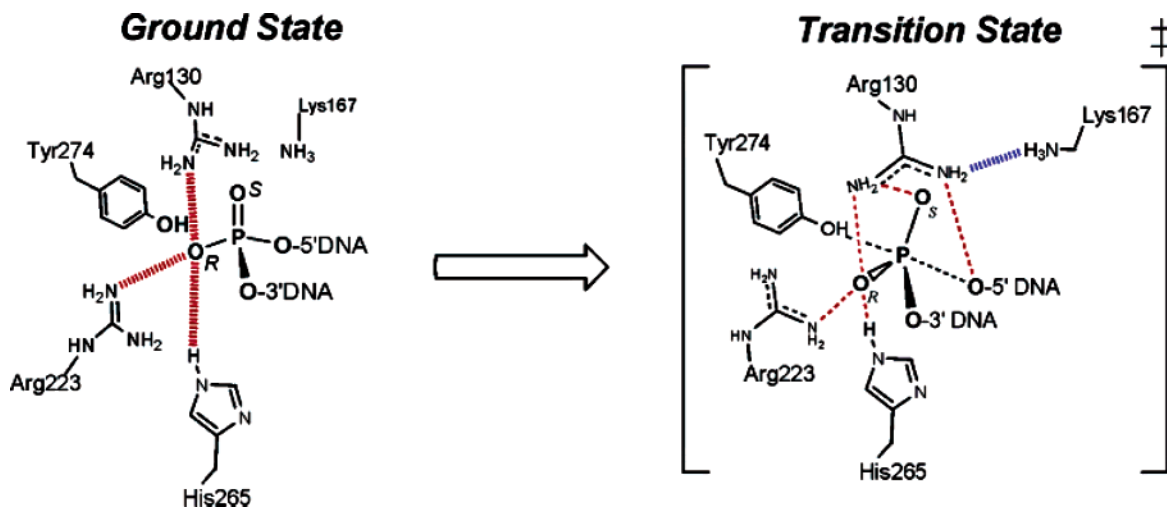


**Figure 17.** Ground-state and transition-state interactions of vTopo with the reactive phosphoryl group as deduced from thio effect and structural studies. Long-range electrostatic interactions in the ground state are indicated with red hashed lines.

Mutations	Interactions Present	Bridging Sulfur Rescue (fold)
A. Wild-type		0.7
B. R130A		190
C. K167A		370
D. R130K		2600
E. R130K:K167A		2000

**Figure 18.** Postulated interactions between Arg130, Lys167, and the 5'-leaving oxygen based on structural studies (1EJ9) and thio effect measurements.<sup>76,88</sup>

The nonbridging thio effect measurements also suggested a revised model for the interactions of Arg130 and Lys167 with the 5'-leaving oxygen (Figure 18). For the wild-type enzyme, Arg130 interacts with both the nonbridging and bridging oxygens: its interaction with the nascent negative charge on the 5'-leaving oxygen is likely enhanced by the presence of Lys167, which could lower the  $pK_a$  of Arg130 so that it more closely matches that of the 5'-hydroxyl group. For wild-type Topo, efficient leaving group stabilization by Arg130 leads to a nonexistent 5'-sulfur rescue. For the R130A mutation, the interaction between Arg130 and Lys167 is abrogated, allowing Lys167 to move within hydrogen bonding distance of the 5' leaving group, thereby acting as

a less efficient surrogate general acid catalyst. Thus, the 5'-sulfur rescue is much greater than that for the wild-type enzyme but 14-fold smaller than the maximal effect seen for the R130K mutant. In the absence of Lys167, Arg130 forms a weaker interaction with the developing negative charge on the leaving oxygen because its  $pK_a$  is no longer optimally matched to the leaving group, resulting in a substantial 5'-sulfur rescue (370-fold) but significantly less than the maximal value observed for R130K. For the R130K mutation (Figure 18), the Lys130 side chain is too short to reach the 5'-bridging oxygen or the nonbridging oxygens, but it is still able to interact with the Lys167 side chain, preventing its adventitious interaction with the 5' oxygen as observed with the R130A mutation. Accordingly, the 5' rescue is largest (2600-fold) for R130K and similar for the R130K:K167A double mutation (2000-fold). Although these interpretations are not without alternatives, they are most consistent with all of the thio effect and structural data. Interestingly, a role for guanidinium groups as general-acid catalysts in phosphoryl transfer has been recently established in a model system.<sup>103</sup>

#### 7.2.4. Methylphosphonate Substitution and VTopo Mutagenesis

Vaccinia topoisomerase is an excellent example where methylphosphonate substitution in the DNA backbone led to useful information about the enzyme mechanism.<sup>104–106</sup> Chemical substitution of the nonbridging phosphoryl oxygens by a methyl group within the consensus CCCTT sequence revealed critical vTopo–DNA contacts required for cleavage by this enzyme. Methyl substitution at eight positions within the recognition sequence had profound deleterious effects on the single-turnover cleavage rate in the range 50- to 50 000-fold (Figure 19).<sup>105</sup> The authors divided the effects into three classes, each with distinct mechanistic interpretations. The first class involved substitutions at the +5 and –2 positions of the scissile strand and at +1 and +2 of the nonscissile strand, all of which had no effect on DNA cleavage. The straightforward interpretation was that the enzyme formed no functionally significant interactions with these positions. The second class consisted of a single substitution at the +4 position of the nonscissile strand which gave rise to a large deleterious effect, but with no stereo-selectivity. One possible interpretation for this outcome is a long-range electrostatic interaction with a cationic group (or

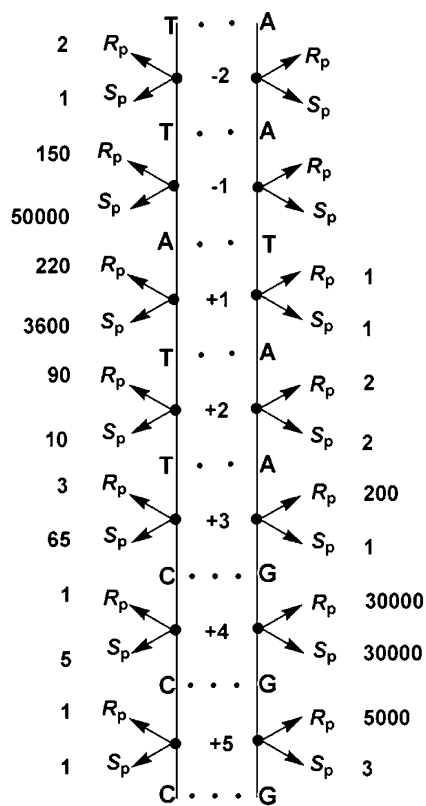


**Figure 19.** Damaging effects (fold) of stereospecific methylphosphonate substitution in the DNA backbone of the vTopo consensus sequence.<sup>91</sup>

groups), because either methylphosphonate diastereomer would equally well ablate the negative charge of the linkage. The third class involved six phosphate groups (-1, +2, +3, and +4 phosphates of the scissile strand and the +3 and +5 phosphates of the non-scissile strand) which showed large deleterious effects for only one methylphosphonate diastereomer. A reasonable interpretation for this outcome was that a stereospecific interaction with one diastereomer was occurring. However, in the absence of structural information on the complex or additional measurements of mutagenesis effects, the details of these interactions remain unknown, although some inferences were derived from inspection of the structure of the human topoisomerase–DNA complex.<sup>88,89</sup>

Shuman and co-workers also made methylphosphonate substitutions at the scissile phosphate linkage and combined these with alanine mutagenesis of active site residues Arg223 and His265.<sup>106</sup> The  $S_p$  and  $R_p$  MeP diastereomers slowed the rate of DNA cleavage by the wild-type enzyme by factors of 220 and 3600, respectively. Both the R223A and H265A mutants showed no further decrease in activity when the *pro*- $S_p$  oxygen was replaced by a methyl group, but they showed large rate decreases when the *pro*- $R_p$  oxygen was replaced. These findings were consistent with the nonbridging thio effect measurements, where Arg223 and His265 were both found to interact with the  $R_p$  sulfur (note that the stereochemical designation is opposite for sulfur and methyl substituents; i.e., the  $R_p$  sulfur is equivalent to a  $S_p$  methyl group). Thus, methylphosphonate and thio effect studies agree remarkably well in this system.

Another interesting outcome from the methylphosphonate substitutions at the scissile linkage was that a latent hydrolytic reaction of the covalent phosphotyrosine linkage was accelerated by ~30 000-fold upon substitution.<sup>104</sup> The authors

proposed that the negative charge of the native phosphodiester linkage electrostatically repelled the nucleophilic water, and consequently, the hydrolysis rate was increased upon substitution with either an  $R_p$  or  $S_p$  methyl group. An alternative explanation is that the hydrolysis rate is increased because of the potentially greater reactivity of methylphosphonate linkages toward nucleophilic attack as compared to that of the phosphodiester.<sup>43,107</sup>

### 7.3. Uracil DNA Glycosylase

The DNA repair enzyme uracil DNA glycosylase (UDG) hydrolytically cleaves the glycosidic bond of deoxyuridine (dUrd) from both single-stranded and duplex DNA using an extrahelical recognition mechanism where the uracil is flipped into the enzyme active site pocket, a process known as “base flipping” (Figure 20).<sup>108–113</sup> Uracil arises in DNA through two independent pathways: the spontaneous deamination of cytosine residues and the misincorporation of dUTP during DNA replication. The primary role of the enzyme in DNA repair is to prevent CG → AT transition mutations.<sup>114</sup> However, UDG is now implicated in many more biological processes as diverse as acquired immunity and viral infectivity.<sup>115,116</sup> The enzymatic process of uracil removal involves a recognition step followed by the chemical step of glycosidic bond cleavage, and both of these steps involve utilization of enzyme interactions with the DNA phosphodiester backbone in very different ways.

The multistep mechanism of uracil flipping involves (i) enzymatic capture of the uracil base as it emerges from the base stack due to normal thermal motions of the base pair,<sup>112</sup> (ii) docking in at least one transient site on the enzyme that is not the active site,<sup>111,117,118</sup> and, finally, (iii) full insertion deep into the active site pocket where catalysis then ensues. Base flipping can be envisioned as having two coupled reaction coordinates: rotation of the base from the duplex stack and bending of the DNA. DNA bending of the DNA backbone is believed to occur ahead of base rotation, and structural studies strongly implicate three serine residues in the bending process, making this an ideal case for using phosphorothioate substitution in combination with enzyme mutagenesis.

Mechanistic and structural studies on UDG have established a remarkable stepwise mechanism for cleavage of the glycosidic bond of dUrd in DNA that involves a positively charged oxocarbenium ion sugar intermediate and a negatively charged uracil leaving group (Figure 20).<sup>119–121</sup> An “electrostatic sandwich” mechanism was proposed in which the cationic sugar was stabilized by the anionic aspartate located beneath the sugar ring and the uracil anion leaving group above the ring (Figure 20).<sup>121</sup> Oxocarbenium ions are extremely unstable chemical species, and UDG is one of only two enzymes in which such an intermediate has been suggested. For UDG, the evidence was quite compelling. Kinetic isotope effect measurements and X-ray crystallography indicated a highly dissociative process with a preorganized planar sugar conformation in the ground-state ES complex and in the glycosyl cation intermediate,<sup>113,120</sup> and structural studies with a 1-azadeoxyribose glycosyl cation mimic provided a structural snapshot of the second addition transition state in which the attacking water molecule was approaching the electropositive 1-position of the sugar.<sup>121</sup> The unstable glycosyl cation intermediate present in the UDG reaction immediately led to questions of whether electrostatic interactions between the positively charged sugar and anionic

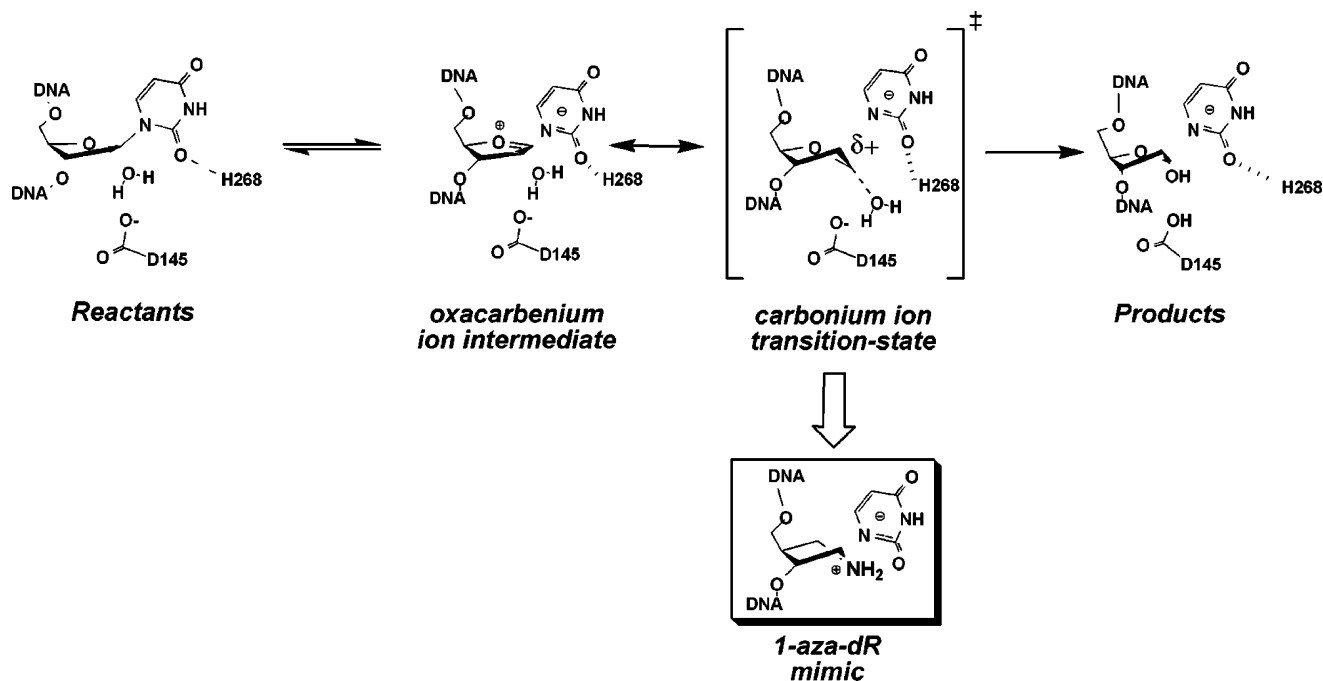


**Figure 20.** Reaction pathway of UDG. A stepwise mechanism has been established involving a discrete oxocarbenium ion intermediate that is stabilized by electrostatic interactions with active site residues and the phosphodiester groups of the DNA. Two catalytic groups are indicated in the figure: His268, which serves as a hydrogen bond donor to stabilize the developing negative charge on uracil O2 in the dissociative transition state, and Asp145, which stabilizes the cationic sugar of the intermediate. The structure of 1-azadeoxyribose (1-aza-dR), which is proposed to mimic the sugar conformation in the second transition state involving water addition, is also shown.

DNA phosphates were used for transition-state stabilization.<sup>122–124</sup> As described below, methylphosphonate substitution provided an excellent experimental approach to test the role of indirect electrostatic interactions of the DNA phosphates with the transition state and, in addition, with a cationic transition-state mimic.<sup>125</sup>

### 7.3.1. Nonbridging Phosphorothioate Substitution near the Deglycosylation Site

The interactions of three serine residues of UDG with the +1, -1, and -2 phosphate positions of the DNA backbone were examined using kinetic thio effects, mutagenesis, and X-ray crystallography.<sup>126</sup> The interactions of UDG with each phosphate group as determined by structural studies are shown in Figure 21A, and the cooperative interaction map deduced from the kinetic measurements is shown in Figure 21B. The experimental findings that supported this interaction map are summarized below. The reader is referred to the energetic definitions in section 4 which are used extensively here.

**Ser88.** Removal of the side chain hydroxyl of Ser88 gave rise to the largest damaging effect of any of the serine residues in the transition state (3.5 kcal/mol). Since Ser88 was known to interact with the +1 *pro-S<sub>p</sub>* oxygen from the structural studies (Figure 21A), it was not surprising that its removal gave rise to a similar damaging effect as removal of the +1 nucleotide (3.7 kcal/mol). The combined analysis of the structural data and the thio and mutational effects on  $k_{cat}/K_m$  indicated that Ser88 forms a stereospecific interaction with the +1 *pro-S<sub>p</sub>* oxygen ( $\Delta G_c = -2$  kcal/mol) and is coupled indirectly to both of the -1 nonbridging oxygens ( $\Delta G_c = +1$  and +1.1 kcal/mol, Table 1). The strongly negative  $\Delta G_c$  at the +1 *S<sub>p</sub>* position reflects the 28-fold smaller thio effect for S88A at this site and is consistent with the direct interaction of this group with the +1 *S<sub>p</sub>* substituent (Figure 21A). In contrast, the strongly positive

$\Delta G_c$  values for the Ser88 interaction with the *S<sub>p</sub>* and *R<sub>p</sub>* -1 positions would not be predicted by inspection of the crystal structure or from studies of the thio effect or mutational effect alone. The positive coupling energy reveals the presence of strain between the Ser88 and the -1 phosphodiester. In this interpretation, when Ser88 or one of the -1 nonbridging oxygens is changed individually, not only a favorable interaction but also an unfavorable strain energy is lost. Thus, each individual change appears less damaging due to the release of strain energy. When the effects of both changes are measured simultaneously (i.e., the reaction of the thio substrate with the mutated enzyme), two favorable interactions are lost, but strain is lost only once, leading to the result that the double effect is more damaging than the sum of the single effects. Strain may result from either electrostatic repulsion between the compressed +1 and -1 phosphodiester groups or conformational strain in the system. As noted in Table 1, this energetic coupling is an example of anticooperativity in binding the transition state.

**Ser189.** The combined analysis of the thio and mutational effects on  $k_{cat}/K_m$  indicated that Ser189 had a strong energetic coupling ( $\Delta G_c$ ) with the +1 *pro-S<sub>p</sub>* oxygen (-1.7 kcal/mol), even though Ser189 does not directly interact with the +1 position as judged by the structure. In addition, the absence of any significant change in the *R<sub>p</sub>* and *S<sub>p</sub>* thio effects at the -1 position upon removal of Ser189 indicated that this group did not interact directly or indirectly with the nonbridging oxygens of the -1 phosphodiester. This result is consistent with the crystal structure, which indicates that the Ser189  $\gamma$ -OH is within hydrogen bonding distance of the 5' *bridging* oxygen at the -1 position (Figure 21A). Taken in conjunction with the Ser88 thio effect studies, the results with S189A indicate a complex pattern of energetic cross-talk between 5' and 3' serine pinching residues and three of the four nonbridging oxygens at the +1 and -1 positions (Figure 21B).

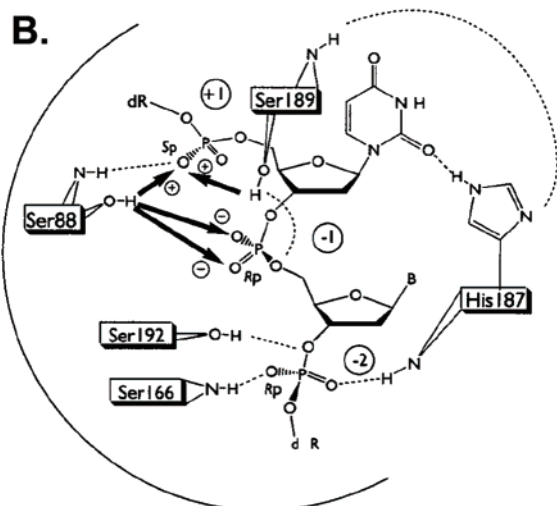
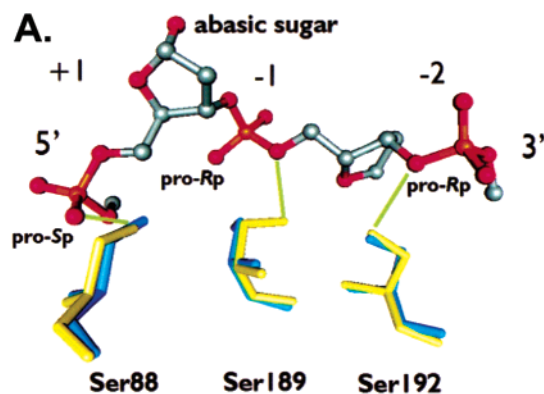


**Figure 21.** Direct and indirect coupling energies between serine side chains and phosphodiester oxygens of UDG. (A) The interactions of UDG with its abasic site DNA product as determined by X-ray crystallography (pdb code 1FLZ, yellow; pdb code 1SSP, blue). The coupling energy may be interpreted as the additional apparent energy of interaction between the phosphodiester oxygen and the given serine residue as compared to that of the interaction with sulfur (Table 1). In this figure, bold arrows with plus and minus signs indicate cooperative and anticooperative coupling energies, respectively. Dashed lines represent hydrogen bonds. The S88A mutation causes an increased  $R_p$  and  $S_p$  thio effect at the  $-1$  position (strain), and the S189A mutation causes a stereoselective decrease in the  $S_p$  thio effect at the  $+1$  phosphodiester (positive cooperativity). The S189A and S192G mutations have little effect on the magnitude of the thio effect at the  $-1$  or  $-2$  position. A highly cooperative network is indicated.

**Ser192.** Removal of Ser192, which interacts with the 3' bridging oxygen of the  $-2$  phosphate in the crystal structure, had an equally damaging effect on the stability of the ES complex and the transition state ( $+1.7$  kcal/mol), indicating that this group has no role in reducing the kinetic barrier  $ES \rightarrow ES^\ddagger$ . The combined analyses of the thio and mutational effects on  $k_{cat}/K_m$  indicated that Ser192 did not interact directly or indirectly with the nonbridging oxygens of the  $-2$  phosphodiester, which was consistent with the crystal structure (Figure 21A). Therefore, the large  $-2 R_p$  thio effect likely results from disruption of the favorable amide hydrogen bond from Ser166 to the  $pro-R_p$  oxygen (Figure 21B). The significantly larger  $R_p$  effect as compared to the  $S_p$  thio effect at the  $-2$  position is consistent with the shorter and presumably stronger hydrogen bond between Ser166 NH and the  $pro-R_p$  oxygen ( $2.75$  Å), as compared to the

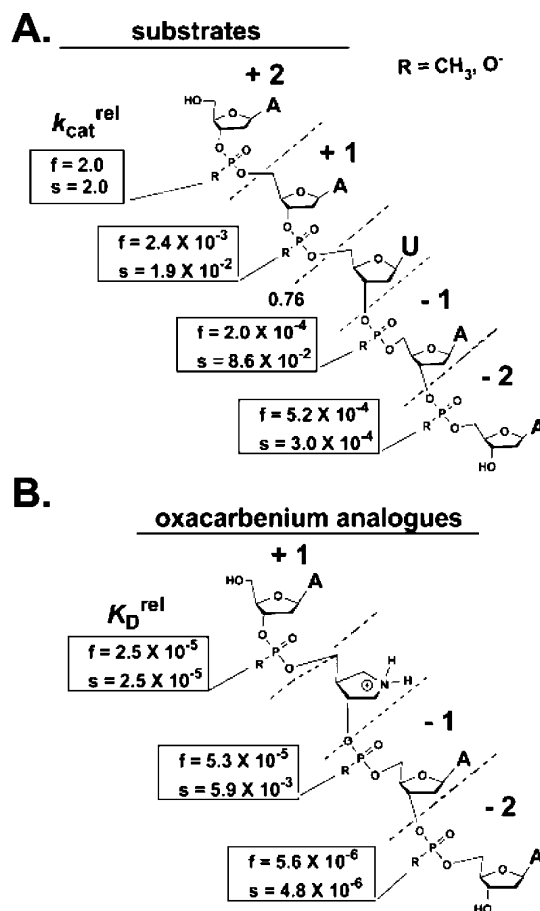


**Figure 22.** Methylphosphonate substitution studies on UDG catalysis and transition-state inhibitor binding. (A) The relative  $k_{cat}$  values for the fast (f) and slow (s) migrating methylphosphonate stereoisomers are indicated. (B) 1-Azadeoxyribose oxocarbenium ion mimics. Each phosphodiester linkage was substituted with a methylphosphonate group to remove the charge, and the relative  $K_D$  values compared to the all phosphodiester analogue were measured.

hydrogen bond between the  $-2 pro-S_p$  oxygen and His187 NH ( $2.99$  Å).

### 7.3.2. Nonbridging Methylphosphonate Substitution near the Deglycosylation Site

A rigorous and novel experimental test of the electrostatic role of DNA phosphate groups in stabilization of the glycosyl cation intermediate was obtained using the tools of synthetic chemistry and free energy correlations.<sup>125</sup> The strategy was to ablate the negative charges on each of the four phosphodiester groups through the use of stereospecific methylphosphonate (MeP) substitutions. Then, the damaging effects of these methylphosphonate substitutions on the kinetic parameters were compared with their damaging effects on binding of a cationic 1-azadeoxyribose oxocarbenium ion analogue (Figure 22). This approach established the relative roles of these anionic phosphate groups in binding the neutral ground state, the cationic transition state, and a stable chemical mimic of the cationic intermediate. The results established that Coulombic interactions with the DNA backbone are a powerful method that enzymes may employ to selectively stabilize a charged transition state over an uncharged ground state. These favorable electrostatic interactions with the substrate may account for the extraordinary stepwise mechanism for glycosidic bond cleavage catalyzed by UDG.



A very powerful application of the data in this study was a plot of  $\log K_D$  for the series of MeP substituted inhibitors against  $\log k_{cat}/K_m$  for the corresponding substrates (Figure 23). This linear correlation had a slope of  $-1$ , indicating

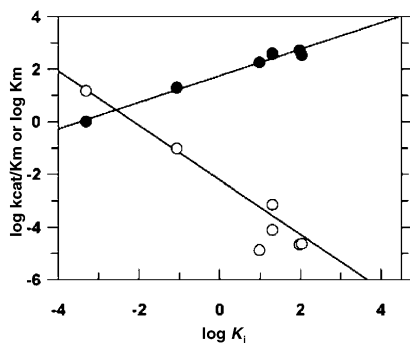


**Figure 23.** Linear free energy correlations for binding of the methylphosphonate substituted 1-azadeoxyribose analogues and deoxyuridine substrates.<sup>111</sup> The empty circles show the correlation between  $\log k_{cat}/K_m$  for the methylphosphonate substituted substrates and  $\log K_D$  for the corresponding methylphosphonate substituted 1-azadeoxyribose analogues. The slope of the line is  $-1$ . The filled circles show the correlation between  $\log K_m$  for the methylphosphonate substituted substrates and  $\log K_D$  for the corresponding MeP substituted 1-azadeoxyribose analogues. The slope of this line is 0.5.

that each of the phosphodiester groups of the DNA has a similar favorable energetic interaction with the transition state and the cationic inhibitor, supporting the conclusion that the transition state has considerable cationic character. In contrast, a linear plot of  $\log K_D$  against  $\log K_m$  showed a slope of only 0.5 (Figure 23). Thus, the phosphodiester groups are used for ground-state stabilization of the substrate as well, but the interactions are weaker than those in the transition state, consistent with the development of favorable electrostatic interactions as the charged transition state is approached.

#### 7.4. Phosphoinositol-Specific Phospholipase C

Phosphatidylinositol-specific phospholipase C (PI-PLC) from *Bacillus thuringiensis* uses a stepwise mechanism to convert phosphatidylinositol into inositol 1,2-cyclic phosphate and then into the final product inositol-1-phosphate (Figure 24).<sup>127</sup> The reaction is reminiscent of ribonuclease A because nucleophilic substitution involves internal attack of the 2-hydroxyl group of the substrate on the adjacent phosphodiester linkage, resulting in a cyclic phosphate intermediate. The products of the mammalian PI-PLC reaction, diacylglycerol and inositol 1,4,5-trisphosphate, play key roles in intracellular signaling processes by activating protein kinase C and intracellular calcium stores, respectively.<sup>128,129</sup> An elegant series of thio effect and mutagenesis experiments by Bruzik and colleagues, combined with

crystallographic studies of a closely related PI-PLC,<sup>130</sup> have led to a detailed picture of the interactions between the substrate and enzyme in the transition state as depicted in Figure 25. The proposed mechanism involves (i) general base

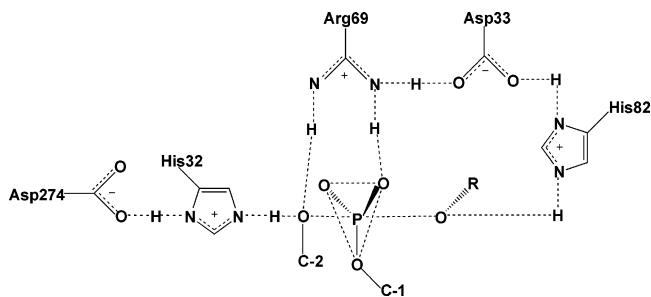


**Figure 25.** Network of coupled interactions deduced from thio effect measurements and structural studies on PI-PLC (see text).

catalysis of C-2 hydroxyl proton removal by the catalytic dyad of Asp274-His32, with assisted positioning of the nucleophile by Arg69, (ii) general acid catalysis of leaving group expulsion by a catalytic triad consisting of His82-Asp33-Arg69, and (iii) transition-state stabilization of the negative charge on the *pro-S<sub>p</sub>* nonbridging oxygen by Arg69. A unique aspect of these studies is how this intricate network of coupled interactions was deduced by well-designed mutagenesis experiments using the nonbridging (DPPsI) and bridging (DPsPI) sulfur versions of the natural substrate dipalmitoylphosphatidylinositol (DPPI) (Figure 26). The

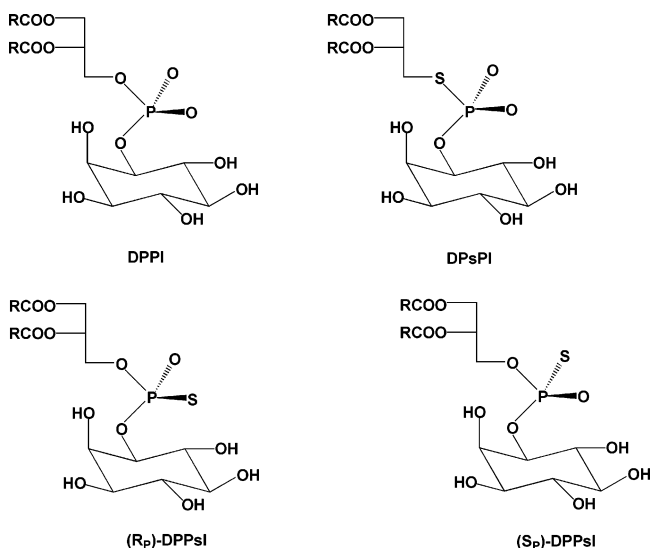


**Figure 26.** Thio substituted substrate analogues for PI-PLC.

findings that led to the proposed interactions and mechanism shown in Figure 25 are described below.

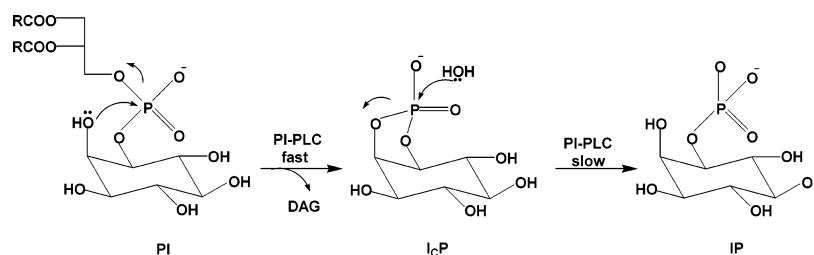


**Figure 24.** Reaction mechanism of phosphatidylinositol-specific phospholipase C (PI-PLC) from *Bacillus thuringiensis*.

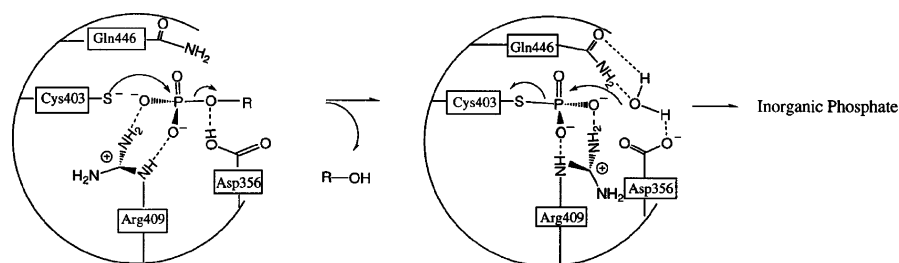


**Figure 27.** Active site interactions and catalytic mechanism of the tyrosine protein kinase from *Yersinia pestis*.<sup>122</sup>

#### 7.4.1. Nonbridging Phosphorothioate Substitution and Mutagenesis

Large mutagenesis effects, strict residue conservation across species, and proximity to a bound inositol product analogue implicated five residues as being critical to catalysis:<sup>131</sup> Asp274 (~0.01%), Asp33 (~0.1%), Arg69 (~0.01%), His32 (~0.001%), and His82 (~0.001%), where the percent activities of the alanine mutants relative to the wild-type enzyme are noted parenthetically. On the basis of its close proximity to the 2-OH group of the substrate and the large effect of the H32A mutation, His32 was proposed as a general base. The large detrimental effect of the D274A mutation, a residue that is too far away for direct contact with the substrate but very close to His32, led to the proposal of a catalytic dyad involving Asp274 and His32. In this type of arrangement, Asp274 could serve to increase the basicity of His32.<sup>132</sup> The proposed interaction of Arg69 with the *pro*-S<sub>p</sub> oxygen was implicated by the 500-fold relaxation of the stereoselectivity of the wild-type enzyme toward the nonbridging phosphorothioate substrate DPPsI when Arg69 was substituted with lysine ( $k_{RP}/k_{Sp}$  values for the wild-type enzyme in the range 8200–30 000 depending on the detergent used in the buffer, whereas R69K showed a ratio  $k_{RP}/k_{Sp} = 16$ ).<sup>133</sup> The enormous nonbridging S<sub>p</sub> thio effect for the wild-type enzyme ( $k_{ox}/k_s \sim 300\,000$ ) is one of the largest ever reported and likely arises from disruption of the network of interactions involving Arg69. The large stereoselective effect has been assigned to transition-state interactions because thio substitution had little effect on ground-state binding.<sup>133</sup> The interaction between Arg69 and Asp33 shown in Figure 25 was indicated by a similar large relaxation of the stereoselectivity upon mutation of Asp33 to Asn or Ala ( $k_{RP}/k_{Sp} = 5\text{--}29$ ).<sup>133</sup> As will be described below, the catalytic network involving Arg69 and Asp33 was elegantly extended to include the proposed general acid, His82, by the use of *dual* bridging and nonbridging thio effect measurements (section 7.4.2).

#### 7.4.2. Combining Bridging and Nonbridging Phosphorothioate Substitution with Mutagenesis

The final interactions in Figure 25 were deduced by using substrate analogues that contained either a single bridging sulfur (DPsPI) or a bridging and nonbridging sulfur (DPsPsI). Crystallography implicated His82 as the general acid for protonating the leaving group,<sup>130</sup> but a role for Asp33 in leaving group protonation was suggested by the enhanced activity of D33A with DPsPI as compared to DPPI.<sup>134</sup> Thus, connectivity was suggested between Asp33 and His82, the direct proton donor. Elegant confirmation of a catalytic triad His82–Asp33–Arg69 was obtained using the phosphorodithioate substrate DpsPsI.<sup>131</sup> The concept is that if these three residues act cooperatively, then alteration of the interactions at the nonbridging oxygens (especially the *pro*-S<sub>p</sub> that

interacts with Arg69) should affect the interactions at the bridging site, and the opposite would also be true. A dramatic demonstration of this expected outcome was realized by comparing the activities of the wild-type enzyme with the substrates DPPsI and DPsPsI. When the S<sub>p</sub> oxygen was substituted with sulfur, a 10<sup>–5</sup>-fold reduction in rate was observed compared to the case of the oxygen substrate, but when the second bridging sulfur was added, the rate increased by 100-fold as compared to the case of S<sub>p</sub>-DPPsI. The observation of interdependence between bridging and nonbridging thio effects provides an orthogonal approach to demonstrate connectivity between Arg69 and His82 that is distinct from mutagenesis.

### 7.5. Protein Tyrosine Phosphatase

Protein tyrosine phosphatases (PTPases) catalyze the removal of the phosphoryl group from phosphotyrosine in peptides and proteins, as well as aryl phosphates.<sup>135</sup> Thus, in conjunction with tyrosine protein kinases, these enzymes determine the steady-state phosphorylation state of many proteins in the cell. This superfamily of enzymes shares a common mechanism for catalysis (Figure 27). In this mechanism, an active site cysteine residue acts as a nucleophile to accept the phosphoryl group of the substrate, thus forming a cysteinyl phosphate intermediate. Formation of the intermediate involves transition-state stabilization by Arg409 and general acid catalysis of aryl leaving group expulsion by Asp356. The second step of the reaction involves attack of a water nucleophile with general base assistance by the same conserved aspartate which gave up its proton in the first step. There are large rate effects upon substitution of an oxygen atom of the substrate with sulfur.<sup>136</sup> Zhang et al. made rate measurements on five PTPases using *p*-nitrophenylphosphate and *p*-nitrophenylphosphorothioate as substrates and observed large thio effects in the range ~100- to 5000-fold. This was striking because phosphate monoesters react 10 to 60 times faster than the phosphorothioate forms.

#### 7.5.1. Nonbridging Phosphorothioate Substitution and Mutagenesis

To understand the basis for the large thio effects with PTPases, a detailed mechanistic investigation was performed.<sup>136</sup> The authors established (i) that chemistry was the rate-limiting step for all substrates, thus ensuring that transition-state information was being revealed, (ii) that the phosphorothioate reaction occurred in the same active site as the phosphate substrate and employed a cysteinyl thio-phosphate intermediate, and (iii) that, using linear free energy correlations, the transition-state structures for the solution and enzymatic reactions with phosphates and phosphorothioates were the same. (Based on  $\beta_{nuc}$  values of about 0.06 and 0.15 for the phosphorothioate and phosphate substrates,

respectively, the solution and enzymatic reactions of phosphorothioates appeared slightly more dissociative than those of the corresponding phosphates.)

Given the similar transition states for the solution and enzymatic reactions but the widely different thio effects, a hypothesis was tested that the large enzymatic thio effects arose from imperfect steric and electrostatic complementarities between the enzyme and the transition state for the phosphorothioate substrate. Consistent with this interpretation, the R409K mutant showed a 54-fold decrease in the thio effect, supporting the direct interaction with the phosphoryl group observed in the crystal structure ( $\Delta G_c = -2.3$  kcal/mol, Table 1). In addition, D356A and W354A showed 8- and 22-fold smaller thio effects. Although Trp354 does not directly interact with the substrate (Figure 27), it is likely important for positioning of Arg409 and Asp356, giving rise to the decreased thio effect ( $\Delta G_c = -1.8$  kcal/mol, Table 1). The authors made the conclusion that, in general, sulfur substitution is likely to have the largest damaging effect in transition states rather than ground states, because of stricter geometric and electrostatic requirements in the transition state. Indeed, they found no thio effect on binding, and the compiled findings in Table 1 strongly support the conclusion that sulfur substitution has much greater damaging effects in the transition state of enzymatic reactions. This fact is evidenced by the strongly negative coupling energies ( $\Delta G_c$ ) for all residues that directly contact a phosphate oxygen *in the transition state*.

## 8. Concluding Remarks

At this time there have been enough measurements of substitution effects, and in some cases combined with mutational effects, to make some general conclusions concerning this methodology. For a reference database, we have compiled all of the sulfur and methyl substitution measurements described in this review in Tables 1 and 2, respectively. The first conclusion to emphasize is that confidence in a proposed mechanism is greatest when a number of diverse measurements have been made, when each measurement provides a consistent view of the mechanism and, in their entirety, they exclude alternative mechanisms. In the cases where thio or methyl effects have been most elucidative, measurements of ground-state structures by crystallography or NMR, measurements of the substitution effect on both the ground-state and transition-state energies, and measurements of the change in the substitution effect upon mutagenesis have been performed. Most importantly, the measurements must be done under appropriate conditions where chemistry is the rate limiting step. Second, as clearly observed in Table 1, thio substitution effects are always damaging in the transition state but may frequently lead to enhanced binding in the ground state. As pointed out by Zhang et al. (section 7.5.1), this likely represents important spatial and electronic differences between the ground state and transition state of enzymatic phosphoryl transfer reactions, with the transition state having much more rigid requirements than the ground state. Third, large stereospecific methyl effects (when present) are always damaging whether in the ground state or transition state and likely represent a direct ionic or hydrogen bond with the substituted oxygen (Table 2). In contrast, nonstereoselective methyl effects may be reasonably interpreted as indicating a nonspecific electrostatic interaction at a given linkage. Finally, coupling energies between oxygen and sulfur ( $\Delta G_c$ , Table 1) fall in

the range  $-5.9$  to  $+1.1$  kcal/mol. Excluding the large  $\Delta G_c$  values for RNase T1 and PI-PLC that arise from disruption of a coupled network of interactions, a mean coupling energy of  $-2 \pm 0.4$  kcal/mol in the transition state is calculated from the remaining 12 interactions that are known to be direct by structural studies ( $\Delta G_c$  values corresponding to direct interactions are bold in Table 1). These combined findings provide an estimate of the net steric and electronic differences between sulfur and oxygen while interacting with a variety of amino acid side chains. The mean value of  $-2$  kcal/mol appears to be insensitive to whether the interaction is electrostatic or, alternatively, is a neutral hydrogen bond. Thus, this amount of coupling energy should be generally expected when single direct interactions are disrupted by sulfur substitution. *It is imperative to recognize that this mean value for  $\Delta G_c$  does not apply to ground-state interactions, which show much less predictable energetic effects of thio substitution (Table 1).* A corollary to this conclusion is that coupling energies significantly larger than this range will generally indicate disruption of a network of interactions in the active site upon substitution. We trust that the compilation of findings and studies discussed in this review will serve as a useful guide for further research using this methodology.

## 9. Abbreviations

2-AP	2-aminopurine
DFT	density functional theory
EcoRI	restriction endonuclease RI
EcoRV	restriction endonuclease RV
PI-PLC	phosphatidylinositol phospholipase C
PTPase	protein tyrosine phosphatase
RNase	ribonuclease
UDG	uracil DNA glycosylase
vTopo	vaccinia topoisomerase

## 10. Acknowledgments

The authors' work was supported by NIH Grants GM56834 and GM68626.

## 11. References

- (1) Huse, M.; Kuriyan, J. *Cell* **2002**, *109*, 275.
- (2) Steeg, P. S.; Palmieri, D.; Ouatas, T.; Salerno, M. *Cancer Lett.* **2003**, *190*, 1.
- (3) Schroeder, G. K.; Lad, C.; Wyman, P.; Williams, N. H.; Wolfenden, R. *Proc. Natl. Acad. Sci., U.S.A.* **2006**, *103*, 4052.
- (4) Downes, C. P.; Gray, A.; Lucocq, J. M. *Trends Cell Biol.* **2005**, *15*, 259.
- (5) Shan, S. O.; Herschlag, D. *Methods Enzymol.* **1999**, *308*, 246.
- (6) Frey, P. A. *Adv. Enzymol. Relat. Areas Mol. Biol.* **1989**, *62*, 119.
- (7) Eckstein, F. *Angew. Chem., Int. Ed.* **1975**, *14*, 160.
- (8) Eckstein, F.; Romaniuk, P. J.; Connolly, B. A. *Methods Enzymol.* **1982**, *87*, 197.
- (9) Eckstein, F.; Gish, G. *Trends Biochem. Sci.* **1989**, *14*, 97.
- (10) Shan, S.; Kravchuk, A. V.; Piccirilli, J. A.; Herschlag, D. *Biochemistry* **2001**, *40*, 5161.
- (11) Shan, S.; Yoshida, A.; Sun, S.; Piccirilli, J. A.; Herschlag, D. *Proc. Natl. Acad. Sci., U.S.A.* **1999**, *96*, 12299.
- (12) Houglund, J. L.; Kravchuk, A. V.; Herschlag, D.; Piccirilli, J. A. *PLoS Biol.* **2005**, *3*, e277.
- (13) Mizuuchi, K.; Nobbs, T. J.; Halford, S. E.; Adzuma, K.; Qin, J. *Biochemistry* **1999**, *38*, 4640.
- (14) Sennikov, P. G. *J. Phys. Chem.* **1994**, *98*, 4973.
- (15) Frey, P. A.; Sammons, R. D. *Science* **1985**, *228*, 541.
- (16) Schwalbe, C. H.; Goody, R.; Saenger, W. *Acta Crystallogr.* **1973**, *29*, 2264.
- (17) Florian, J.; Strajbl, M.; Warshel, A. *J. Am. Chem. Soc.* **1998**, *120*, 7959.
- (18) Shan, S. O.; Herschlag, D. *Proc. Natl. Acad. Sci., U.S.A.* **1996**, *93*, 14474.
- (19) Shan, S. O.; Loh, S.; Herschlag, D. *Science* **1996**, *272*, 97.



- (20) Dantzman, C. L.; Kiessling, L. L. *J. Am. Chem. Soc.* **1996**, *118*, 11715.
- (21) Bruice, T. C.; Benkovic, S. J. *Bioorganic Mechanisms*; W. A. Benjamin: New York, 1966.
- (22) Admiraal, S. J.; Herschlag, D. *Chem. Biol.* **1995**, *2*, 729.
- (23) Creighton, T. E. *Proteins*; W.H. Freeman and Co.: New York, 1997.
- (24) Thiviyanathan, V.; Vyazovkina, K. V.; Gozansky, E. K.; Bichenchova, E.; Abramova, T. V.; Luxon, B. A.; Lebedev, A. V.; Gorenstein, D. G. *Biochemistry* **2002**, *41*, 827.
- (25) Mukherjee, S.; Bhattacharyya, D. *Biopolymers* **2004**, *73*, 269.
- (26) Smith, J. S.; Nikonowicz, E. P. *Biochemistry* **2000**, *39*, 5642.
- (27) Miller, P. S.; Dreon, N.; Pulford, S. M.; Mcparland, K. B. *J. Biol. Chem.* **1980**, *255*, 9659.
- (28) Lesnikowski, Z. J.; Jaworska, M.; Stec, W. J. *Nucleic Acids Res.* **1990**, *18*, 2109.
- (29) StraussSoukup, J. K.; Maher, L. J. *J. Biol. Chem.* **1997**, *272*, 31570.
- (30) StraussSoukup, J. K.; Rodrigues, P. D.; Maher, L. J. *Biophys. Chem.* **1998**, *72*, 297.
- (31) Kirby, A. J.; Varvogli, Ag. *J. Chem. Soc. B: Phys. Org.* **1968**, 135.
- (32) Kirby, A. J.; Younas, M. J. *Chem. Soc. B: Phys. Org.* **1970**, 1165.
- (33) Khan, S. A.; Kirby, A. J. *J. Chem. Soc. B: Phys. Org.* **1970**, 1172.
- (34) Anderson, M. A.; Shim, H.; Raushel, F. M.; Cleland, W. W. *J. Am. Chem. Soc.* **2001**, *123*, 9246.
- (35) Hengge, A. C. *FEBS Lett.* **2001**, *501*, 99.
- (36) Humphry, T.; Forconi, M.; Williams, N. H.; Hengge, A. C. *J. Am. Chem. Soc.* **2002**, *124*, 14860.
- (37) Grzyska, P. K.; Czyryca, P. G.; Purcell, J.; Hengge, A. C. *J. Am. Chem. Soc.* **2003**, *125*, 13106.
- (38) Sorensen-Stowell, K.; Hengge, A. C. *J. Org. Chem.* **2005**, *70*, 4805.
- (39) Milstien, S.; Fife, T. H. *J. Am. Chem. Soc.* **1967**, *89*, 5820.
- (40) Herschlag, D.; Piccirilli, J. A.; Cech, T. R. *Biochemistry* **1991**, *30*, 4844.
- (41) Catrina, I. E.; Hengge, A. C. *J. Am. Chem. Soc.* **2003**, *125*, 7546.
- (42) Purcell, J.; Hengge, A. C. *J. Org. Chem.* **2005**, *70*, 8437.
- (43) Hudson, R. F.; Keay, L. J. *Chem. Soc.* **1956**, 2463.
- (44) Zhang, Y.-L.; Hollfelder, F.; Gordon, S. J.; Chen, L.; Keng, Y.-F.; Wu, L.; Herschlag, D.; Zhang, Z.-Y. *Biochemistry* **1999**, *38*, 12111.
- (45) Williams, N. H.; Wyman, P. *Chem. Commun.* **2001**, 1268.
- (46) Haake, P. C.; Westheimer, F. H. *J. Am. Chem. Soc.* **1961**, *83*, 1102.
- (47) Mildvan, A. S.; Weber, D. J.; Kuliopulos, A. *Arch. Biochem. Biophys.* **1992**, *294*, 327.
- (48) Wells, J. A. *Biochemistry* **1990**, *29*, 8509.
- (49) Eckstein, F. *Angew. Chem., Int. Ed.* **1983**, *22*, 423.
- (50) Herschlag, D.; Cech, T. R. *Biochemistry* **1990**, *29*, 10159.
- (51) Stivers, J. T.; Shuman, S.; Mildvan, A. S. *Biochemistry* **1994**, *33*, 327.
- (52) Iyer, R. P.; Egan, W.; Regan, J.; Beaucage, S. L. *J. Am. Chem. Soc.* **1990**, *112*, 1253.
- (53) Grasby, J. A.; Connolly, B. A. *Biochemistry* **1992**, *31*, 7855.
- (54) Lesser, D. R.; Grajkowski, A.; Kurpiewski, M. R.; Koziolkiewicz, M.; Stec, W. J.; Jen-Jacobson, L. *J. Biol. Chem.* **1992**, *267*, 24810.
- (55) Mag, M.; Luking, S.; Engels, J. W. *Nucleic Acids Res.* **1991**, *19*, 1437.
- (56) Burgin, A. B. *Methods Mol. Biol.* **2001**, *95*, 119.
- (57) Burgin, A. B., Jr.; Nash, H. A. *Curr. Biol.* **1995**, *5*, 1312.
- (58) Kwon, K.; Jiang, Y. L.; Song, F.; Stivers, J. T. *J. Biol. Chem.* **2002**, *277*, 353.
- (59) Wozniak, L. A.; Pyzowski, J.; Wieczorek, M.; Stec, W. J. *J. Org. Chem.* **1994**, *59*, 5843.
- (60) Smith, S. A.; McLaughlin, L. W. *Biochemistry* **1997**, *36*, 6046.
- (61) Reynolds, M. A.; Arnold, L. J.; Almazan, M. T.; Beck, T. A.; Hogrefe, R. I.; Metzler, M. D.; Stoughton, S. R.; Tseng, B. Y.; Trapane, T. L.; Tso, P. O. P.; Woolf, T. M. *Proc. Natl. Acad. Sci., U.S.A.* **1994**, *91*, 12433.
- (62) Schell, P.; Engels, J. W. *Tetrahedron Lett.* **1998**, *39*, 8629.
- (63) Cleland, W. W. *Adv. Enzymol. Relat. Areas Mol. Biol.* **1977**, *45*, 273.
- (64) Cleland, W. W. *CRC Crit. Rev. Biochem.* **1982**, *13*, 385.
- (65) Dertinger, D.; Uhlenbeck, O. C. *RNA* **2001**, *7*, 622.
- (66) Dertinger, D.; Behlen, L. S.; Uhlenbeck, O. C. *Biochemistry* **2000**, *39*, 55.
- (67) Valegard, K.; Murray, J. B.; Stonehouse, N. J.; vandenWorm, S.; Stockley, P. G.; Liljas, L. *J. Mol. Biol.* **1997**, *270*, 724.
- (68) Potter, B. V.; Eckstein, F. *J. Biol. Chem.* **1984**, *259*, 14243.
- (69) Olsen, D. B.; Kotzorek, G.; Eckstein, F. *Biochemistry* **1990**, *29*, 9546.
- (70) Kurpiewski, M. R.; Koziolkiewicz, M.; Wilk, A.; Stec, W. J.; Jen-Jacobson, L. *Biochemistry* **1996**, *35*, 8846.
- (71) Rosenberg, J. M. *Curr. Opin. Struct. Biol.* **1991**, *1*, 104.
- (72) Thorogood, H.; Grasby, J. A.; Connolly, B. A. *J. Biol. Chem.* **1996**, *271*, 8855.
- (73) Winkler, F. K.; Banner, D. W.; Oefner, C.; Tsernoglou, D.; Brown, R. S.; Heathman, S. P.; Bryan, R. K.; Martin, P. D.; Petratos, K.; Wilson, K. S. *EMBO J.* **1993**, *12*, 1781.
- (74) Jeltsch, A.; Pleckaityte, M.; Selent, U.; Wolfes, H.; Siksnys, V.; Pingoud, A. *Gene* **1995**, *157*, 157.
- (75) Herschlag, D. *J. Am. Chem. Soc.* **1994**, *116*, 11631.
- (76) Glennon, T. M.; Warshel, A. *J. Am. Chem. Soc.* **1998**, *120*, 10234.
- (77) Breslow, R.; Chapman, W. H., Jr. *Proc. Natl. Acad. Sci., U.S.A.* **1996**, *93*, 10018.
- (78) Thompson, J. E.; Venegas, F. D.; Raines, R. T. *Biochemistry* **1994**, *33*, 7408.
- (79) Loverix, S.; Winqvist, A.; Stromberg, R.; Steyaert, J. *Chem. Biol.* **2000**, *7*, 651.
- (80) Loverix, S.; Winqvist, A.; Stromberg, R.; Steyaert, J. *Nat. Struct. Biol.* **1998**, *5*, 365.
- (81) Stivers, J. T.; Harris, T. K.; Mildvan, A. S. *Biochemistry* **1997**, *36*, 5212.
- (82) Kwon, K.; Stivers, J. T. *J. Biol. Chem.* **2002**, *277*, 345.
- (83) Kwon, K.; Nagarajan, R.; Stivers, J. T. *Biochemistry* **2004**, *43*, 14994.
- (84) Nagarajan, R.; Kwon, K.; Nawrot, B.; Stec, W. J.; Stivers, J. T. *Biochemistry* **2005**, *44*, 11476.
- (85) Sekiguchi, J.; Shuman, S. *J. Biol. Chem.* **1994**, *269*, 31731.
- (86) Wittschieben, J.; Shuman, S. *J. Biol. Chem.* **1994**, *269*, 29978.
- (87) Shuman, S. *Biochim. Biophys. Acta* **1998**, *1400*, 321.
- (88) Stewart, L.; Redinbo, M. R.; Qiu, X.; Hol, W. G.; Champoux, J. J. *Science* **1998**, *279*, 1534.
- (89) Redinbo, M. R.; Stewart, L.; Kuhn, P.; Champoux, J. J.; Hol, W. G. *Science* **1998**, *279*, 1504.
- (90) Redinbo, M. R.; Champoux, J. J.; Hol, W. G. *Curr. Opin. Struct. Biol.* **1999**, *9*, 29.
- (91) Redinbo, M. R.; Stewart, L.; Champoux, J. J.; Hol, W. G. *J. Mol. Biol.* **1999**, *292*, 685.
- (92) Champoux, J. J. *Ann. N. Y. Acad. Sci.* **2000**, *922*, 56.
- (93) Redinbo, M. R.; Champoux, J. J.; Hol, W. G. *Biochemistry* **2000**, *39*, 6832.
- (94) Krogh, B. O.; Shuman, S. *Mol. Cell* **2000**, *5*, 1035.
- (95) Krogh, B. O.; Shuman, S. *J. Biol. Chem.* **2002**, *277*, 5711.
- (96) Kanavarioti, A.; Rosenbach, M. T. *J. Org. Chem.* **1991**, *56*, 1513.
- (97) Kanavarioti, A.; Rosenbach, M. T.; Hurley, T. B. *Origins Life Evol. Biosphere* **1991**, *21*, 199.
- (98) Kanavarioti, A.; Bernasconi, C. F.; Doodokyan, D. L.; Alberas, D. J. *J. Am. Chem. Soc.* **1989**, *111*, 7247.
- (99) Hanna, R. L.; Gryaznov, S. M.; Doudna, J. A. *Chem. Biol.* **2000**, *7*, 845.
- (100) Gryaznov, S. M.; Winter, H. *Nucleic Acids Res.* **1998**, *26*, 4160.
- (101) Chen, Y.; Narendra, U.; Iype, L. E.; Cox, M. M.; Rice, P. A. *Mol. Cell* **2000**, *6*, 885.
- (102) Stivers, J. T.; Jagadeesh, G. J.; Nawrot, B.; Stec, W. J.; Shuman, S. *Biochemistry* **2000**, *39*, 5561.
- (103) Piatek, A. M.; Gray, M.; Anslyn, E. V. *J. Am. Chem. Soc.* **2004**, *126*, 9878.
- (104) Tian, L.; Claeboe, C. D.; Hecht, S. M.; Shuman, S. *Mol. Cell* **2003**, *12*, 199.
- (105) Tian, L.; Claeboe, C. D.; Hecht, S. M.; Shuman, S. *Structure* **2004**, *12*, 31.
- (106) Tian, L.; Claeboe, C. D.; Hecht, S. M.; Shuman, S. *Structure* **2005**, *13*, 513.
- (107) Forconi, M.; Herschlag, D. *J. Am. Chem. Soc.* **2005**, *127*, 6160.
- (108) Stivers, J. T.; Pankiewicz, K. W.; Watanabe, K. A. *Biochemistry* **1999**, *38*, 952.
- (109) Jiang, Y. L.; Song, F.; Stivers, J. T. *Biochemistry* **2002**, *41*, 11248.
- (110) Jiang, Y. L.; Stivers, J. T. *Biochemistry* **2002**, *41*, 11236.
- (111) Krosky, D. J.; Song, F.; Stivers, J. T. *Biochemistry* **2005**, *44*, 5949.
- (112) Cao, C.; Jiang, Y. L.; Stivers, J. T.; Song, F. *Nat. Struct. Mol. Biol.* **2004**, *11*, 1230.
- (113) Parikh, S. S.; Walcher, G.; Jones, G. D.; Slupphaug, G.; Krokan, H. E.; Blackburn, G. M.; Tainer, J. A. *Proc. Natl. Acad. Sci., U.S.A.* **2000**, *97*, 5083.
- (114) Stivers, J. T.; Jiang, Y. L. *Chem. Rev.* **2003**, *103*, 2729.
- (115) Unniraman, S.; Fugmann, S. D.; Schatz, D. G. *Science* **2004**, *305*, 1113.
- (116) Priet, S.; Gros, N.; Navarro, J. M.; Boretto, J.; Canard, B.; Querat, G.; Sire, J. *Mol. Cell* **2005**, *17*, 479.
- (117) Krosky, D. J.; Schwarz, F. P.; Stivers, J. T. *Biochemistry* **2004**, *43*, 4188.
- (118) Jiang, Y. L.; McDowell, L.; Poliks, B.; Studelska, D.; Cao, C.; Potter, G. S.; Schaefer, J.; Song, F.; Stivers, J. T. *Biochemistry* **2004**, *43*, 15429.
- (119) Jiang, Y. L.; Drohat, A. C.; Ichikawa, Y.; Stivers, J. T. *J. Biol. Chem.* **2002**, *277*, 15385.
- (120) Werner, R. M.; Stivers, J. T. *Biochemistry* **2000**, *39*, 14054.
- (121) Bianchet, M. A.; Seiple, L. A.; Jiang, Y. L.; Ichikawa, Y.; Amzel, L. M.; Stivers, J. T. *Biochemistry* **2003**, *42*, 12455.
- (122) Dinner, A. R.; Blackburn, G. M.; Karplus, M. *Nature* **2001**, *413*, 752.



- (123) Jiang, Y. L.; Stivers, J. T. *Biochemistry* **2001**, *40*, 7710.
- (124) Jiang, Y. L.; Stivers, J. T. *Biochemistry* **2003**, *42*, 1922.
- (125) Jiang, Y. L.; Ichikawa, Y.; Song, F.; Stivers, J. T. *Biochemistry* **2003**, *42*, 1922.
- (126) Werner, R. M.; Jiang, Y. L.; Gordley, R. G.; Jagadeesh, G. J.; Ladner, J. E.; Xiao, G.; Tordova, M.; Gilliland, G. L.; Stivers, J. T. *Biochemistry* **2000**, *39*, 12585.
- (127) Kravchuk, A. V.; Zhao, L.; Kubiak, R. J.; Bruzik, K. S.; Tsai, M. D. *Biochemistry* **2001**, *40*, 5433.
- (128) Berridge, M. J. *Nature* **1993**, *365*, 388.
- (129) Berridge, M. J. *Nature* **1993**, *361*, 315.
- (130) Heinz, D. W.; Ryan, M.; Bullock, T. L.; Griffith, O. H. *EMBO J.* **1995**, *14*, 3855.
- (131) Kubiak, R. J.; Yue, X.; Hondal, R. J.; Mihai, C.; Tsai, M. D.; Bruzik, K. S. *Biochemistry* **2001**, *40*, 5422.
- (132) Hondal, R. J.; Zhao, Z.; Kravchuk, A. V.; Liao, H.; Riddle, S. R.; Yue, X.; Bruzik, K. S.; Tsai, M. D. *Biochemistry* **1998**, *37*, 4568.
- (133) Kubiak, R. J.; Hondal, R. J.; Yue, X. J.; Tsai, M. D.; Bruzik, K. S. *J. Am. Chem. Soc.* **1999**, *121*, 488.
- (134) Hondal, R. J.; Bruzik, K. S.; Zhao, Z.; Tsai, M. D. *J. Am. Chem. Soc.* **1997**, *119*, 5477–5478.
- (135) Stoker, A. W. *J. Endocrinol.* **2005**, *185*, 19.
- (136) Zhang, Y. L.; Hollfelder, F.; Gordon, S. J.; Chen, L.; Keng, Y. F.; Wu, L.; Herschlag, D.; Zhang, Z. Y. *Biochemistry* **1999**, *38*, 12111.

CR050317N